



LIBRARY Michigan State University

This is to certify that the

thesis entitled

Biomechanical Analysis of Slipped Capital Femoral Epiphysis with Single and Double Screw Fixation

presented by

Robert Martin Doane

has been accepted towards fulfillment of the requirements for

Master's __degree in __Engineering Mechanics

Date _5-4-90

PLACE IN RETURN BOX to remove this checkout from your record. TO AVOID FINES return on or before date due.

DATE DUE	DATE DUE	DATE DUE

MSU Is An Affirmative Action/Equal Opportunity Institution

in part.

BIOMECHANICAL ANALYSIS OF SLIPPED CAPITAL FEMORAL EPIPHYSIS WITH SINGLE AND DOUBLE SCREW FIXATION

Ву

Robert Martin Doane

A THESIS

Submitted to
Michigan State University
in partial fulfillment of the requirements
for the degree of

MASTER OF SCIENCE

Department of Metallurgy, Mechanics and Materials Science

College of Engineering

1990

Line State of the Control of the Con

60554

BIOMECHANICAL ANALYSIS OF SLIPPED CAPITAL FEMORAL EPIPHYSIS WITH SINGLE AND DOUBLE SCREW FIXATION

Βv

Robert Martin Doane

This study developed an experimental bovine Slipped Capital Femoral Epiphysis (SCFE) model. Structural stiffness of the fixed epiphysis was examined comparing single versus double bone screws. A significant decrease was found for post-fixation tests. Only a 33% average increase in gross stiffness was found with double over single fixation (p<0.05). No statistical difference (p>0.05) was found in stiffness between single and double fixation in the $\underline{in\ vivo}$ range of loading.

The study also examined the structural stability of single and double screw finite element models. The double screw model stiffness was 45 percent higher than the single screw model. When the diameter of the single screw model was increased from 4.5 mm to 5.5 mm, the structural stiffness approached that of the experimental data for double screw fixation. This suggests that an optimum sized single screw fixator may be biomechanically equivalent to two screws, thereby, reducing the chances of surgical complications.

menda di Santa di San

ueta (

This thesis is dedicated to:

Val, whom I met while working on my Master's degree, and was the best thing that happened to me. She has always given me her love, friendship and support

My parents, for all their support and encouragement throughout my years in college.

My advisor, Dr. Roger Haut, for the support and advising in my graduate program. He was always there to answer any questions.

ACKNOWLEDGEMENTS

I would like to acknowledge:

The Fund for Medical Research and Education, Wayne State University, for financial support of this project.

Dr. Arthur Manoli, II, Dr. Lori A. Karol and Dr. Sam F. Cornicelli at The Department of Orthopaedic Surgery, Wayne State University, for their assistance in the clinical aspects of this study.

The College of Osteopathic Medicine at Michigan State
University, for financial assistance and experimental
facilities.

My thesis committee members, Dr. Roger Haut, Dr. Nicholas Altiero and Dr. Curtis Probst, for their time and effort in reviewing my thesis.

TABLE OF CONTENTS

Title P	age
LIST OF TABLES	vi
LIST OF FIGURES	vii
I. INTRODUCTION	
A. Clinical Review	1
B. Hip Biomechanics Review	14
C. SCFE Biomechanics Review	18
II. METHODS AND MATERIALS	
A. Experimental	25
B. Finite Element Analysis	35
IV. RESULTS	
A. Experimental	42
B. Finite Element Analysis	50
V. DISCUSSION	
A. Experimental	54
B. Finite Element Analysis	56
APPENDICES	
A. Experimental Test Data	63
B. Finite Element Code	65
REFERENCES	72

LIST OF TABLES

Table	ge
1. Atypical SCFE Abnormalities 5	
2. Heyman and Herndon Classification 9	
3. Reported Bone Moduli 3	9
4. Intact Epiphyseal Plate Structural Responses 4	5
5. Experimental and FEM Stiffness Data 5	0
6. SCFE Initial Test Data 6	3
7. Single Fixation Test Data 6	4
8. Double Fixation Test Data 6	4
9. Single Screw ANSYS Finite Element Code 6	5
10. Double Screw ANSYS Finite Element Code 6	8

LIST OF FIGURES

Figu	Figure	
1.	Proximal Femur	1
2.	Epiphyseal Plate Radiograph	3
3.	Chronic SCFE	6
4.	Acute SCFE	6
5.	Heterotopic Bone on Screw Head	12
6.	Static Loading on the Hip	15
7.	Hip Force Vectors	16
8.	Loading on the Hip During Slow Gait	17
9.	Proximal Femur Loading	18
10.	Free-Body Diagram of Femoral Epiphysis	19
11.	3-D Loading on the Proximal Femur	20
12.	Resultant Angles on the Hip During Gait $\ldots\ldots$	21
13.	Asnis Screw	26
14.	SCFE Inducing Fixture	27
15.	Bovine Femora Radiograph	28
16.	Bovine Femur Mold	29
17.	Two-Piece Mold	30
18.	Potted Femoral Head	30
19.	Epiphyseal Plate Diameter	31
20.	SCFE Specimen in Testing Machine	32
21.	SCFE Specimen in Testing Machine	33

Figu:	re	Pag
22.	Post-Fixation Radiograph	. 34
23.	Simply Supported Beam	. 35
24.	Single Screw FEM	. 37
25.	Sectioned Single Screw FEM	. 38
26.	Double Screw FEM	. 39
27.	FEM Boundary Conditions	. 41
28.	Bovine Slipped Epiphysis in Fixture	. 42
29.	Epiphyseal Plate	. 43
30.	Typical Load-Deformation Curve	. 43
31.	Diameter Versus Failure Load	. 45
32.	Diameter Versus Average Shear Strength	. 46
33.	Highly Calcified Specimen	. 46
34.	Normally Calcified Specimen	. 47
35.	Internal Fixation Radiograph	. 48
36.	Typical Initial and Fixation Responses $\ldots\ldots\ldots$. 48
37.	Average Initial and Fixation Responses $\ldots\ldots\ldots$. 49
38.	Experimental and FEM Responses	. 51
39.	FEM Single Screw Stresses	. 51
40.	FEM Double Screw Stresses	. 52
41	Single Screw FEM Ontimization	53



I. INTRODUCTION

A. Clinical Review

The epiphyseal plate of the developing femoral head and neck is a weak point in the immature human skeleton and is often injured (Figure 1). As a result, the condition of Slipped Capital Femoral Epiphysis (SCFE) can occur. SCFE is defined as a translocation of the upper femoral head away from its normal anatomical position on the neck. There is

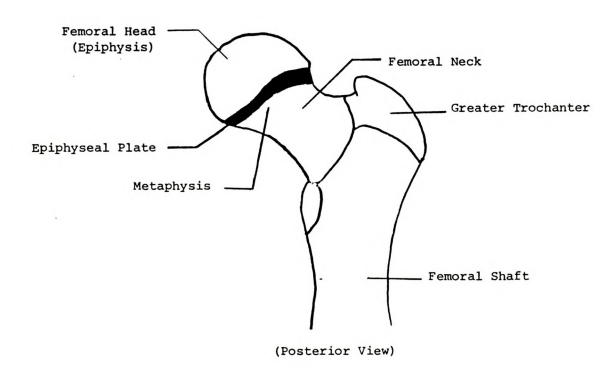


Figure 1. Proximal Femur

no question that this situation can result in permanent deformity if not quickly and properly corrected. SCFE occurs mainly in overweight children from 8 to 15 years and has been known to affect approximately 10 cases per 100,000



population. The left hip is slightly more involved than the right, and bilateral slippage occurs in 25% or more of cases. Simultaneous bilateral slips are rare, but in cases progressing to bilateral involvement, the second slip usually follows within one year 44.

A long bone grows by mitotic duplication of the columns of chondroblasts within the growing cartilage network. In turn, these chondroblasts mature into adult chondrocytes and begin to secrete extracellular cartilaginous matrix. Thus, the enlargement of the growing bone in length and breadth is a process occurring in living tissue and not in the bone itself. Non-living apatite crystals are laid upon an equally extracellular collagen and proteoglycan matrix. When growth of cartilage is complete, the following wave of ossification invades the cartilage by extension of blood vessel loops.

Unlike articular cartilage, growth cartilage has a blood supply, whether in the diaphyseal, metaphyseal, or epiphyseal area. All long bones begin as a cartilaginous anlage, in which the primary center sweeps up the shaft of the growing bone, gradually catching up with the epiphysis 12. During the later stages of this process, mesenchymal cells enter the epiphysis to form a secondary ossification center³⁷. In the epiphysis, cartilage cells proliferate, enlarge, and are replaced by bone in steps similar to those above. Some cartilage cells retain their capacity for growth, forming the epiphyseal plate. Towards the later part of adolescence, the epiphyseal plate is all that



remains within the whole length of bone of the original cartilaginous anlage and therefore, becomes the weak link in calcification of metaphysis to epiphysis (growth plate closure). The epiphyseal plate, which is less dense to radiographs than fully developed bone, is observed as a thin line between the metaphysis and epiphysis (Figure 2).

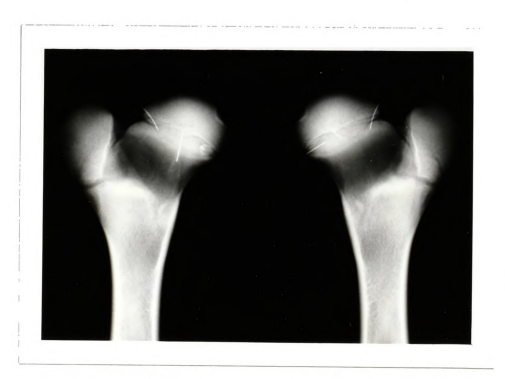


Figure 2. Epiphyseal Plate Radiograph

Epiphyseal fusion does not occur immediately after the epiphysis has calcified. Many children undergo a last spurt of growth. This process of growth is brought to an end by a gradual build-up of circulating levels of sex hormones that cause maturation of secondary sex characteristics. The growth stops and sex hormones act directly on the growing cartilage resulting in final ossification and closure of the epiphyseal plate, therefore, fusing epiphysis to diaphysis.



Fusion may occur any time between 14 to 17 years of age. Closure is characterized by no marked division of epiphysis and metaphysis in radiographs. In the final phase of growth the epiphyseal plate is vulnerable due to the rapidly increasing weight of the individual, increasing muscle bulk and marked transfer of forces through the femur¹². If the stresses through the femoral neck cause shear forces that exceed the strength of materials constituting the epiphyseal plate region, the femoral head will begin to shift. Other atypical factors associated with SCFE are summarized by McAfee²⁶ in Table 1.

The typical case presents itself as a male between 12 to 15 years of age, who is suffering from delayed sexual maturation characterized by obesity, increased height, and deficient gonadal development (Adiposogenital Syndrome). Testosterone deficiency allows continued stimulation of epiphyseal growth by pituitary growth hormones with delayed epiphyseal fusion. Delayed ossification during this period of increasing body mass leads to a form of creep deformation of the epiphyseal plate cartilaginous matrix. This is known as a chronic slip. In other cases, a widened degenerative layer of the growth plate increases vulnerability to sudden shearing stresses, leading to an acute slip and separation of the femoral head. Slips are classified into grades. Grade 1 is a displacement of up to one third of the diameter of the metaphysis. Grade two is between one third and two thirds, and grade three is greater than two thirds of the metaphyseal diameter 12.



Acromegaly and gigantism Chemotherapeutic agents Chorionic gonadotropin therapy Chronic subdural hematomas with Simmond's disease Coxa vara Cryptorchidism Down's syndrome Growth hormone therapy Hemosiderosis-panhypopituitarism Hypoestrogenic states hypergonadotrophic hypogonadism Hypothyroidism, primary and secondary; congenital hypothyroidism (cretinism) and primary acquired hypothyroidism (juvenile myxedema) Klinefelter's syndrome Parathyroid adenomas Pituitary tumors Radiation therapy Renal osteodystrophy Tumors causing chiasmal compression

A chronic slip is characterized by a "parrot beak" deformity (Figure 3). Shortening of the leg as much as 5 cm can arise if not treated. The result is the formation of coxa vara with associated external rotation of the neck, and hyperextension. At no time has there ever been a true break in the continuity of the bone. The pathologic state may be one of repeated minor stress fractures through the matrix of the epiphyseal plate and metaphysis, each being too small to constitute clinical disruption. As a result of this insidious nature of development, the patient continues to walk, but with increasing limp and experiences very slight symptoms. The typical "beak" of subperiosteal bone forms and may give rise to further complications 12.

An acute slip is of the nature of a stress fracture and



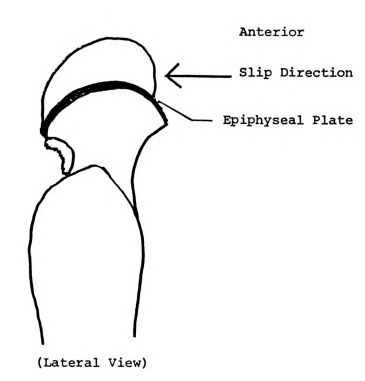


Figure 3. Chronic SCFE

Posterior

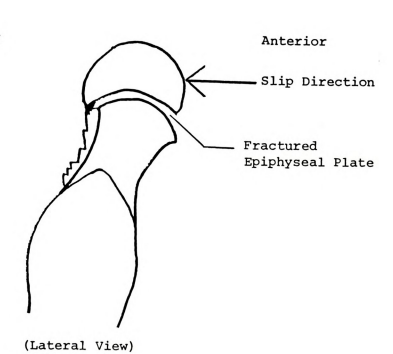
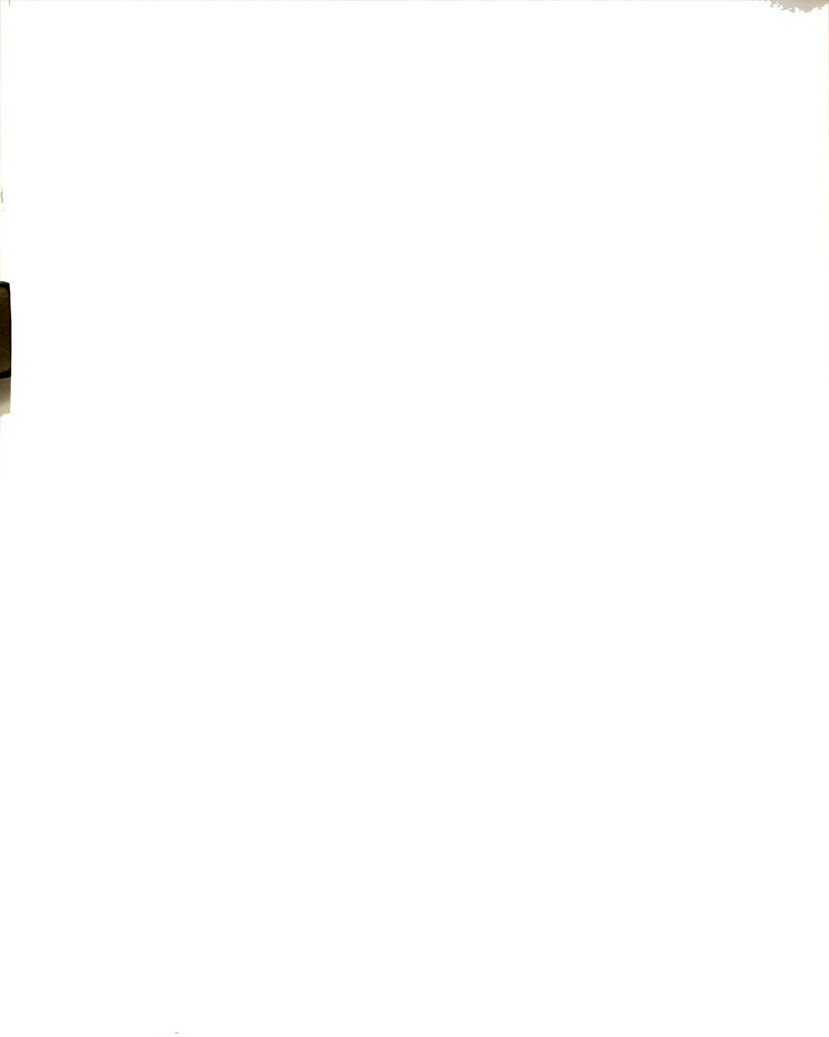


Figure 4. Acute SCFE



is usually the result of a sudden intense force applied to the femoral head (Figure 4). Pathologically, the epiphysis has separated from the upper end of the metaphysis and the shear has occurred through the layer of degenerating cartilage within the growth plate. The epiphyseal plate fractures are usually classified as Salter type I or type II. A Salter type I fracture is clean with no bone fragments attached. Salter type II fractures have metaphyseal bone attached with the epiphysis, thus the fracture has occurred through the epiphyseal plate and through the surrounding cancellous bone. Because of the lack of osseous continuity, the patient is unable to bear weight on the limb. Resulting conditions of coxa vara, external rotation and hyperextension are similar to that of

The most common presentation of SCFE is of a sudden "acute" slip on an underlying "chronic" condition. Clinically, the leg is shortened, adducted, externally rotated and hyperextended. The radiographs reveal epiphyseal disruption with parrot beak callus and widening and distortion of the metaphysis. The acuteness of the slip causes a severe displacement of the femoral head due to the pre-slipped condition of the chronic element. In some patients, the process is gradual and is left untreated. In the end epiphyseal fusion results, but the patient is left with a short, distorted leg. Problems of chondrolysis may result due to the uneven distribution of stresses on the femoral head 12.

a chronic slip 12.

Treatment seems necessary in conditions of SCFE, as Ordeberg 34 et. al. found in Sweden, that in 35 untreated cases of grade 3 slipping, 28 (80%) had some degree of chondrolysis with 12 classified as bone attrition. It was later found by Hägglund 14 et. al., that fixation in situ of SCFE presented better results regarding chondrolysis, pain, walking and degree of motion, than no primary treatment 34 , closed reduction and hip spica 35 or femoral neck osteotomy 13 .

No matter what state the femoral head is in after the epiphyseal plate has displaced, acute, chronic or acute on chronic, further slipping of the epiphyseal plate is possible provided it has not closed. Operation is obligatory to prevent further slipping. In most cases, fixation can be done by inserting pins, nails, or screws from the greater trochanter up the femoral neck into the head. In chronic slips, the creeping metaphysis requires fixation in the position that has been reached (in situ), since no possibility of reduction exists. In the acute slip, it may be possible to reduce the head onto the top of the metaphysis, provided this is done very gently and within a short time of the initial slip. Many orthopedic surgeons agree that pinning is the treatment of choice for mild to moderate slipping 12,14,22,24,29,48, open epiphysiodesis, femoral neck and subtrochanteric osteotomies are performed for severe slipping 12,13,24,28,48, although O'Brien and Fahev³³ reported that 10 of 12 patients with moderate to severe slips of the epiphysis showed satisfactory remodeling



In the early use of pin fixation, complications arose from the Smith-Peterson nail as well as other large triflanged nails due to the separation of the epiphysis as reported by Herndon¹⁸, Jerre¹⁹, and Wilson⁴⁷. Hall¹⁵, Jerre²⁰ and Wilson⁴⁷ have also reported subtrochanteric fractures through the lateral cortex of the neck after penetration by the nail. Inadequate fixation across the physis secondary to premature extrusion from the head due to growth of the femoral neck has also been observed by Jerre¹⁹, and Wilson⁴⁷. It is generally agreed that nailing has been abandoned^{22,48} due to these factors, as well as higher incidence of avascular necrosis¹². As a result, better pin shapes and techniques have been developed.

Various pins such as Knowles, Gouffon, Heggie, Moore, A-M , Zimmer and Asnis are currently used for internal fixation of SCFE. Zahrawi⁴⁸, using 4 to 5 inch Zimmer pins, found good or excellent results in 92% of 61 hips. His

Table 2. Heyman and Herndon Classification

Excellent	- No pain, no limp, normal range of motion
Good	- No pain, no limp, slight limitation of internal rotation beyond neutral position
Fair	- No pain, no limp, slight limitation of abduction as well as external rotation
Poor	 Slight pain after strenuous exercise, mild limp, slight limitation of internal rotation, abduction and flexion
Failure	 Pain with activity, limp, and marked limitation of motion reconstructive surgery required for progressive roentgenographic changes in the hip.



patients were classified by the stringent Heyman Herndon hip classification used by many authors (Table 2).

Carev 6 recently found that the use of Vitallium Knowles pins, promoted growth plate closure and prevented further slip. Lynch²⁴ also recently found that various threaded pin fixations provided acceptable results (Heyman-Herndon grades: excellent, good, fair, or poor) in 83% of 29 patients. Unacceptable results or failures were directly related to preoperative manipulation and/or pin penetration. Moreau²⁹ noted that 68% of 28 hips, with moderate to severe SCFE, showed signs of remodeling with resorption of the superior exposed neck. He justified pinning as a simple, rapid and effective method of treatment allowing remodeling even in more severe slips. Gruebel Lee 12 has successful results with three Knowles pins placed in triangulation within the epiphysis. This implies that the pins are not placed up the femoral neck parallel with each other, but that their points diverge.

There is no question that internal fixation is effective for treatment of SCFE, as $Zahrawi^{48}$ found that pinning <u>in situ</u> is faster, less traumatic, with less bleeding and shorter hospital stay than open epiphysiodesis. But there are still complications that have been noted, such as avascular necrosis leading to the question of pin number and placement, and pin penetration into the joint which can cause chondrolysis. To avoid avascular necrosis, Carey found that best results were achieved using two or three threaded pins placed into the posteroinferior segment of the



femoral head. With this placement, the anterosuperior vascular supply to the femoral head and neck will not be interrupted. Stambough 42 also found that a varus pin position resulting in a more inferior pin placement in the epiphysis was associated with a lower incidence of necrosis and chondrolysis. He found that this occurred when the pin tip was greater than 2.5 mm away from subchondral bone.

Avascular necrosis has also been found to arise as a result of preoperative manipulation (closed reduction). Carey⁶ believes that the nature of SCFE involves disruption of the anterosuperior vasculature of the neck. Attempts at manipulative reduction, before operation, may place in jeopardy the remaining extraosseous vascular supply to the head. In fact, Lynch²⁴ found a direct correlation of avascular necrosis to preoperative manipulation. In 23% of Lynch's patients who went through reduction, necrosis occurred. Zahrawi⁴⁸ found similar results in 3 of 19 hips that were manipulated prior to surgery.

Complications with screw removal also occur. Screws are usually extracted within one year. During this time, the deposition of new cortical trabeculae is firmly adherent to the surface of the bone. If the screw deviates from a perfect spiral, irregular bone is deposited between the threads, making it difficult to remove 12. Another problem which can occur in a pin such as the Knowles or Asnis is that the hexagonal nut that is used for compression of the epiphysis may become buried in subperiosteal bone. It may be necessary to excavate the bone for removal. In another



related bone screw study, bone overgrowth has been observed in canine specimens after only fourteen weeks (Figure 5).



Figure 5. Heterotopic Bone on Screw Head

Gruebel Lee¹² suggests thickening the nut, so it stands away from bone overgrowth. He also suggests that the Knowles pin would be greatly improved if it were cannulated, so that the depth of the pin could be easily measured and its direction ascertained.

With regard to pin penetration, it has been noted by Lynch²⁴ that 31% of his patients with pin penetration (39% of total patients) were failures as classified by Heyman and Herndon. He noted no unacceptable results in patients without pin penetration. This leads to a direct correlation to pin penetration and unacceptable results. Greenough¹¹ found an overall 34% complication rate with multiple screw



fixation procedures. Sixty-four percent of these complications were pin penetration. ${\rm Moss}^{30}$ and Walters 46 have also linked chondrolysis to pin penetration. In many cases the pin penetration goes unnoticed. Nuzzo 32 attributes this to detail loss in x-rays and failure to obtain specific x-ray orientation with the axis of the capital epiphysis. He suggests better operative procedures to reduce these predispositions.

Lehman²² has proposed a new method to detect and prevent pin penetration. He has developed a method of radiographic dye injection through a cannulated screw. A guide wire is first inserted into the assumed correct position for the screw. The screw is then inserted and the wire removed. Die is then injected through the screw and radiographs are taken. If die is found to diffuse into the joint space, the screw is removed and a more desirable placement is obtained.

The obvious way to prevent pin penetration is to prevent it. It logically follows that the fewer pins used in the fixation of SCFE, the less risk that a single pin will violate the articular surface. Stambough 42 et. al., studied the effects of pin placement and number on the incidence of joint penetration. They found that the incidence of complications from in situ pinning with one, two, three and four pins was 0, 5, 12, and 25 percent respectively. The probability of a complication increased significantly with the number of pins. They also asserted that more accurate pin placement is possible when using



fewer pins. Others have found that single pin fixation using an AO screw decreases the incidence of joint penetration by a factor of three 4 .

Aronson and Carlson¹ prospectively studied a series of patients in whom SCFE, both acute and chronic, were treated with a single pin fixation. Twenty-six consecutive slipped epiphyses were treated with a single Asnis screw, including four acute slips. Good or excellent results were obtained in 96% of the children. Pin penetration occurred in just one hip. They concluded that single pin fixation was technically simpler and successful in minimizing the risk of joint penetration. Mann²⁵ retrospectively reviewed thirty-six hips pinned with a single screw. He found an 11% incidence of complications with this technique, and a 2.8% incidence of pin penetration into the hip joint.

It is apparent that a great interest has arisen in the area of single pin fixation of SCFE. Although the clinical results of this type of fixation have been reported, there are limited data on the biomechanical stability of single screw fixation.

B. Hip Biomechanics Review

To analyze the biomechanics of SCFE and internal fixation we must first review the biomechanics of the hip. Tönnis 45 examines the forces comprising the total resultant vector R on the femoral head (Figure 6). Where R is related to the total pressure on the semi-spherical contact surface



of the joint. In this analysis, loading is assumed to be static, as in the stance phase of slow gait, and oriented only in the frontal plane. Cartilaginous responses are neglected.

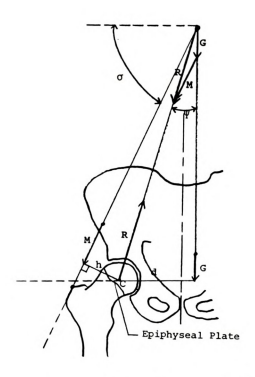
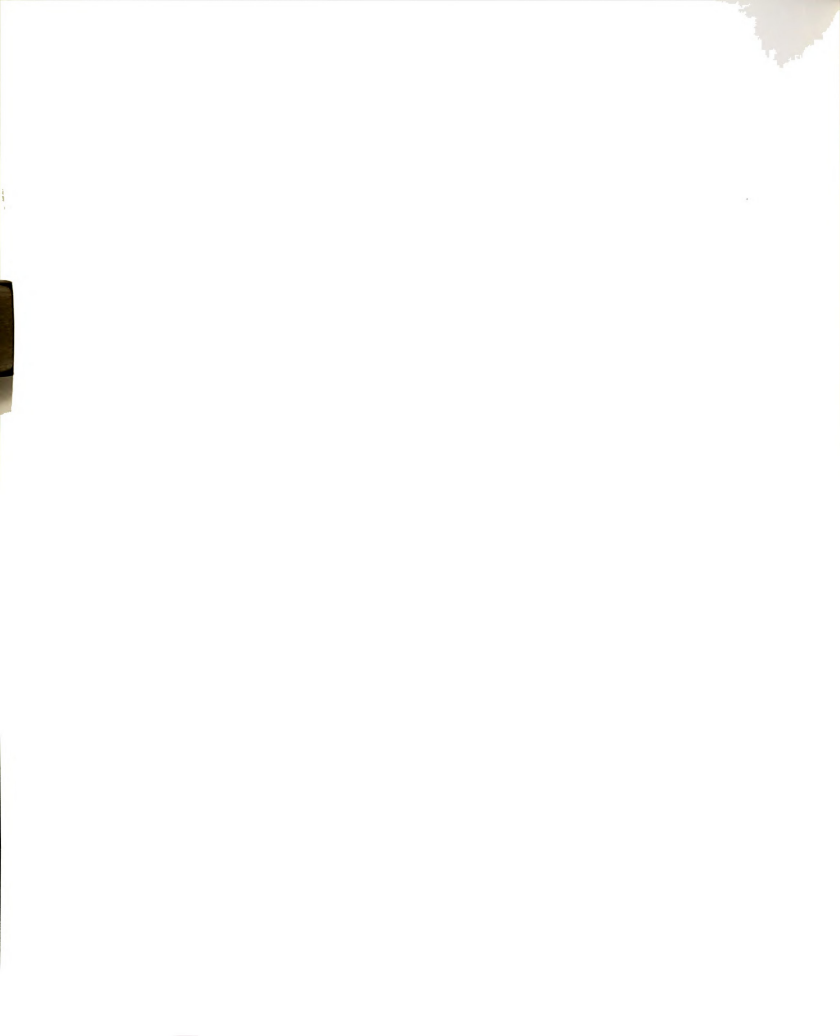


Figure 6. Static Loading on the Hip

The resultant force is comprised of both body loading and internal muscular forces. When the body is in two-legged stance, R depends on body loading only. In one-legged stance, such as in slow gait, R (Equation 1) depends on body loading, G, and muscular forces, M. Where G is the partial body weight at the shifted center of gravity and is comprised of the head, trunk, two arms and opposite leg. M is the resultant force vector due to the hip abductors which balance the moment about the femoral head and keep the pelvis from sagging.



$$R = G + M \tag{1}$$

with moment equation

$$h \times M = d \times G. \tag{2}$$

Summing the forces in the vertical and horizontal directions (Figure 7)

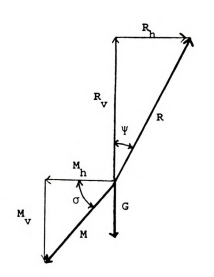


Figure 7. Hip Force Vectors

$$R_{xx} = M_{xx} + G \tag{3}$$

$$R_{h} = M_{h} \tag{4}$$

or

$$R\cos \Psi = M\sin \sigma + G \tag{5}$$

$$Rsin \Psi = Mcos\sigma \tag{6}$$

Substituting for M and reducing

$$R = \frac{G\cos\sigma}{\cos(\Psi + \sigma)}.$$
 (7)



The angles ψ and σ are obtained from standard AP radiographs. In a normal, healthy hip they are listed in Tönnis 45 (reported by Pauwels) as

$$\Psi = 16$$
 , $\sigma = 69$

and from ${\tt TSnnis}^{45}$ (reported by Debrunner, 1975), the weight of one leg is 1/6 of the total body weight. Therefore, the partial body weight is calculated as

$$G = 5/6W \tag{8}$$

where W is total body weight.

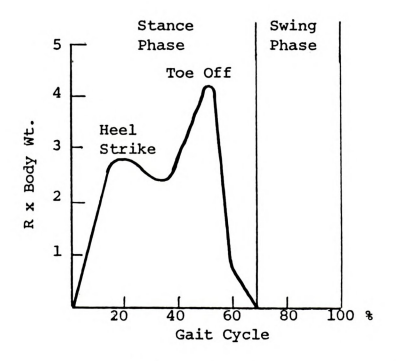


Figure 8. Loading on the Hip During Slow Gait

Thus, equation 7 provides a simple means of calculating the



total resultant force R on the femoral head. Given the above values, R is computed to be $4.11\ \text{times}$ body weight.

Paul³⁶ has experimentally analyzed the magnitude of force through the hip for slow, normal and fast level walking. Using a force plate dynamometer and five of six equilibrium equations, he calculated the resultant force through the hip during the stance phase of gait. The maximum magnitude of loading through the hip was found to be approximately 4 times body weight and occurs midway in the gait cycle (Figure 8). This compares favorably to the calculations from Tönnis.

C. SCFE Biomechanics Review

Chung^{7,8} has analyzed the two-dimensional shear force

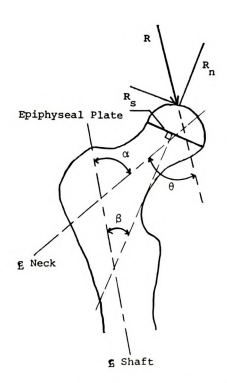
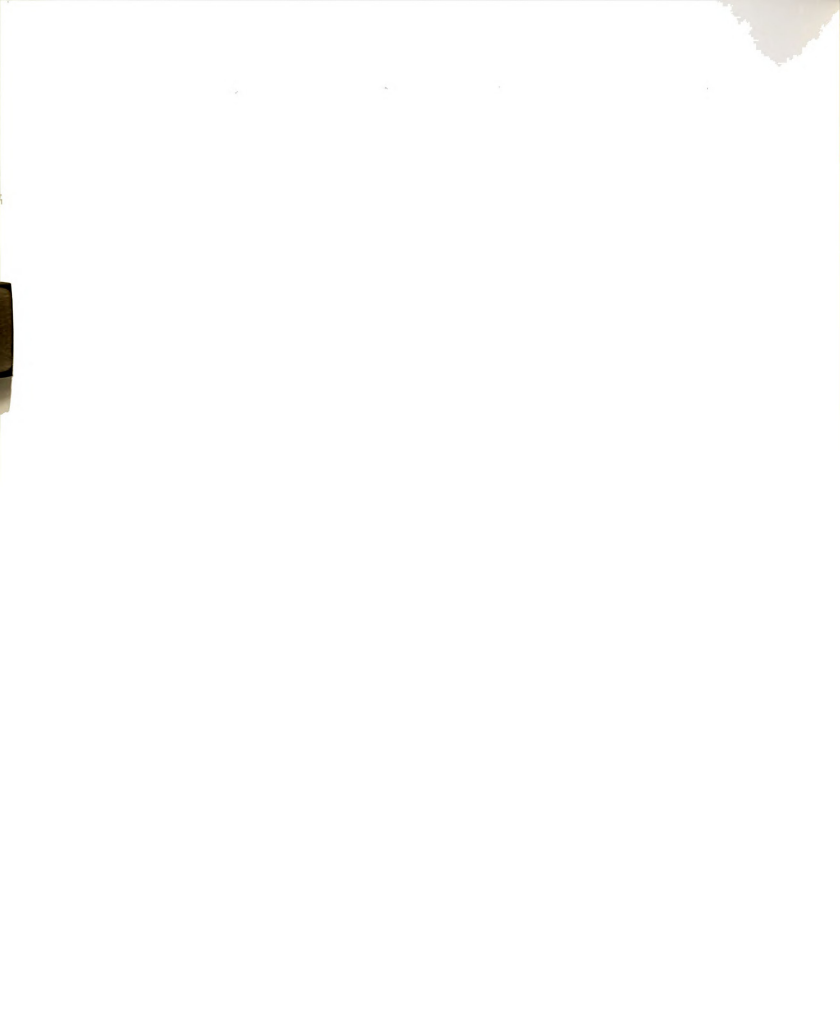


Figure 9. Proximal Femur Loading



on the epiphyseal plate due to the total resultant force R (Figure 9). The neck-shaft angle is given as α , plate-shaft angle as β and resultant force R-neck angle as θ . These angles are easily found from standard AP radiographs. The shear force, as a function of the three angles, is given by

$$R_s = R \sin(\theta + \beta - \alpha)$$
. (9)

As R and/or θ increase so does R_S and the magnitude of the resultant force required to fail the epiphyseal plate decreases. If R_S suddenly exceeds the yield strength of the materials in the epiphyseal plate, acute SCFE occurs. If the process is one of small fractures and regrowth over a period of time, then a chronic SCFE situation exists. Figure 10 shows a free-body diagram of stresses acting on

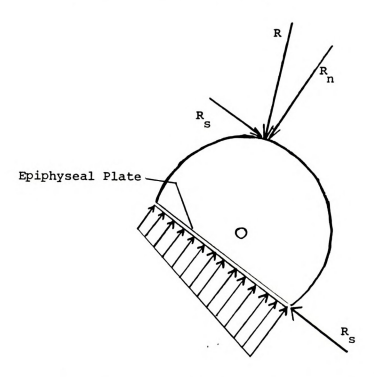
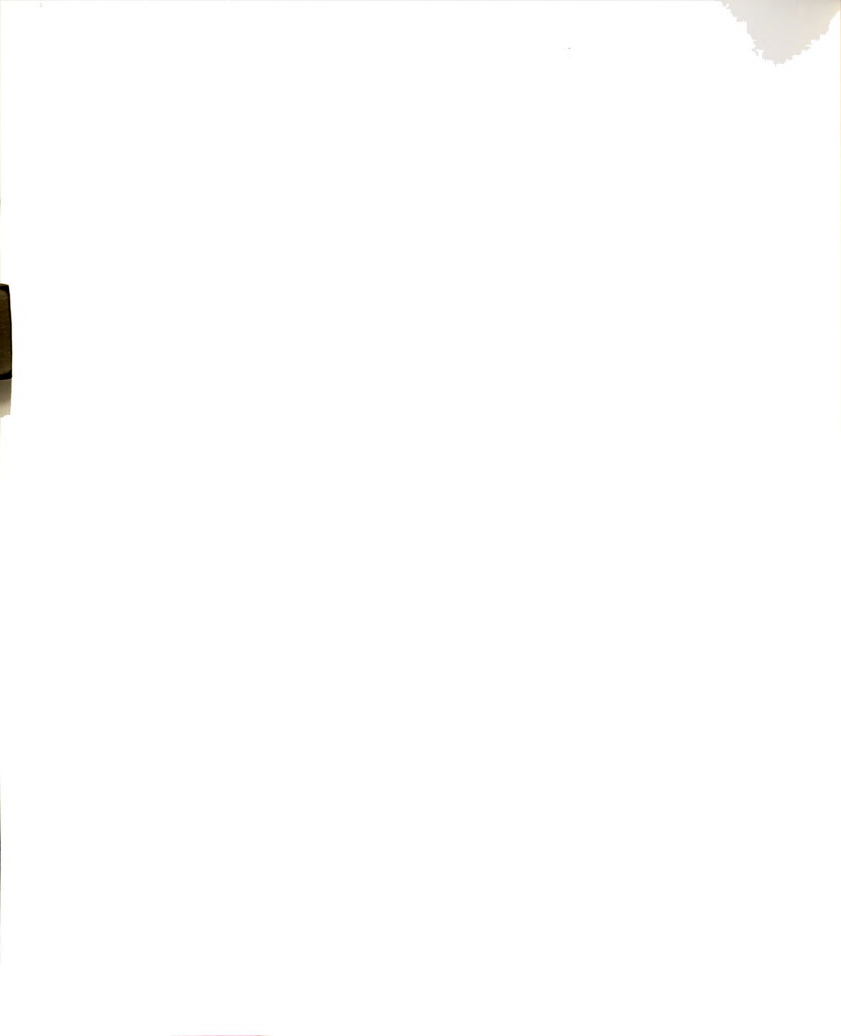


Figure 10. Free-Body Diagram of Femoral Epiphysis



the capital femoral epiphysis.

Litchman and Duffy 23 , using Chung's 7 two-dimensional analysis for the shear force on the epiphyseal plate, calculated the magnitude of shear for the three-dimensional case. Tönnis 45 has stated that R is angled in the frontal plane where it runs medial to lateral downward and in the sagittal plane (perpendicular to the plane of the paper), where it runs anterior to posterior downward relative to the femoral axis. Given this fact, they calculated shear forces in three directions based on their orthogonal coordinate system in which the y and z axes lie in the plane of the epiphyseal plate and the x-axis is normal to its plane (Figure 11). They resolved R into a two-dimensional force

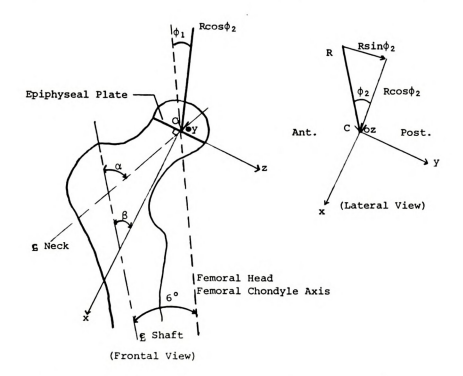


Figure 11. 3-D Loading on the Proximal Femur

in the x-z plane, $R\cos \phi_2$, and resolved this further into the



x and z directions arriving with the equations

$$R_{\perp} = R\cos\phi_2\cos(\beta - 6^0 - \phi_1) \qquad (10)$$

$$R_{_{V}} = R \sin \phi_2 \tag{11}$$

$$R_{\pi} = R\cos\phi_2 \sin(\beta - 6^{\circ} - \phi_1) \tag{12}$$

and the total magnitude of shear force

$$R_{s} = (R_{y}^{2} + R_{z}^{2})^{1/2}$$
$$= R(1-\cos^{2}\phi_{z}\cos^{2}(\beta-6^{0}-\phi_{1}))^{1/2}. (13)$$

The angle of 6° between the femoral shaft-condyle axis and the femoral head-condyle axis was found in a cadaver. The angle β is obtained from standard AP radiographs. The angles ϕ_2 and ϕ_1 during gait, can be found in Paul³⁶ (Figure 12) (Note that ϕ_2 is approximated as the angle between R and

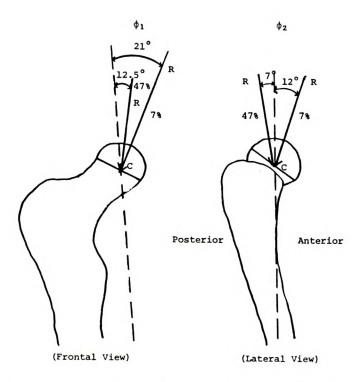


Figure 12. Resultant Angles on the Hip During Gait



the femoral head-condyle axis). At 7% of the stride (heel strike) $\phi_2 = -12^{\circ}$ and $\phi_1 = 21^{\circ}$, while at 47% of the stride (toe off) $\phi_2 = 7^{\circ}$ and $\phi_1 = 12.5^{\circ}$.

Chunq⁷ experimentally examined the shear strength of the human epiphyseal plate among children and adolescents. Twenty-five pairs of human femora from age five days to fifteen years were obtained. The specimens were cleared of all soft tissue and the perichondrial fibrocartilaginous complex was excised in one specimen of each pair. Pins and roentgenograms were obtained to locate the epiphyseal plate. Cross-sectional areas epiphyseal plate and of the perichondrial complex were calculated by counting one millimeter squares enclosed by a tracing on graph paper. A iig was designed with a cylinder shaped, steel loading ram to create the epiphyseal fractures. The proximal neck, trochanter and shaft was stabilized in the fixture with two steel clamps.

Specimens were aligned in the fixture so that the epiphyseal plate was exactly parallel to the loading ram and clamped down. The epiphyseal plates were taken to failure at a rate of 2 mm/min. in the anteroposterior direction. There were many types of failure modes noted. Salter type I and II fractures of the epiphyseal plate were the most common, but Chung also recorded complications such as five neck fractures, one trochanteric fracture, five greenstick bending fractures at the neck, and in three cases the ram punched into the epiphysis. These specimens were ignored in the data analysis.



The shear strength was calculated for each specimen as the failure load divided by the total cross-sectional area of the epiphyseal plate. Chung found that the shear strength (τ) was a function of age with a linear regression correlation coefficient of 0.79

$$\tau = 0.644 + 0.054 \times Age in Years (MPa)$$
. (14)

The shear load was compared for unexcised specimens and excised specimens in each pair. Chung found that excision of the perichondrial complex greatly reduces the total shear load, especially in younger children. By using data from select specimens and equation 9, he calculates shear loads at failure for control femurs of 5.8 and 7.1 times body weight. Chung concludes that the resistance of the epiphyseal plate to shear could be exceeded during normal activities, especially with overweight children and that SCFE may be mechanical in nature.

The only known experimental study, to date, of the biomechanics of SCFE internal fixation, has been Kruger²¹ et. al, who performed a biomechanical comparison of single versus double Steinmann pin fixation in 1988. Forty-four immature canine femora were harvested and all soft tissue was completely removed. The perichondrial fibrocartilaginous complex was resected. The femora were potted in a cylinder which was mounted to a materials testing machine, so that the plane of the epiphyseal plate was parallel to the loading direction. Thus, the epiphysis



received a direct anteroposterior shear to create an acute epiphyseal fracture. The epiphysis was displaced at a rate of 20 mm/min. Of the 44 specimens, 16 failed to fracture at the epiphyseal plate and were rejected. All but two of the remaining specimens failed in a brittle fashion at the yield point.

After the initial fracture, 2 mm Steinmann pins were inserted in a retrograde manner into the femoral head and neck, and clipped flush to the articular surface of the femoral head. Single and double pin fixation was compared using yield load and tangent stiffness data. In reloading the specimens to failure, they found that the intact physis was significantly stiffer (130 ±80 N/mm) than single pin fixation (90±50 N/mm), and no significant difference was found between the intact physis and double pin fixation (110 ±70 N/mm). Two pin fixation yielded a 22% increase in stiffness as compared to single pin fixation. Kruger concluded that multiple pin fixation is superior for treating acute SCFE.

The purpose of this study was fourfold. First, to develop a reproducible SCFE model. Second, to obtain the biomechanical characteristics of the intact epiphyseal plate and compare single and double Asnis screw fixation after inducing SCFE. And finally, develop a mathematical model of the experiment with the potential to optimize the single screw fixation method.



II. METHODS AND MATERIALS

A. Experimental

In designing this study, attempts were made to simulate the clinical situation of adolescent, acute SCFE whenever possible. Bovine immature femora were selected for two reasons. First, the calf proximal femur is only slightly larger than the adolescent proximal femur. Pritchett and Perdue³⁸ examined fifty normal and fifty SCFE patients. They found that the mean diameter of the epiphyseal plate in the normal group was 44.6 mm. In the SCFE patients, the average diameter was 43.9 mm. The range of epiphyseal plate diameter in bovine calf specimens is approximately 45 to 50 mm. Secondly, SCFE has been known to occur in calves¹⁷. The perichondrial fibrocartilaginous complex was left intact, since Chung⁷ found that the shear strength of the human epiphyseal plate was dependent on the integrity of this complex.

The Asnis screw system² (Howmedica, Rutherford, New Jersey) was used in this study. This system is routinely used in the treatment of SCFE. The screws were inserted by a surgeon in the same manner as in the human and the same size screws were used. They were advanced, on the average, four threads past the physis as compared to protruding the joint surface in previous studies²¹. The Asnis screw (Figure 13) has a 6.4 mm buttress thread diameter, 20 mm in length and advances 2.5 mm per revolution. It is a





Figure 13. Asnis Screw

cannulated screw with a shank outer diameter of 4.5 mm and inner diameter of 1.6 mm. The screw is inserted with the aid of a 4 mm reamer and guide pin assembly. Once the reamer is inserted in place, the guide pin is tapped into the bone and the outer sleeve is removed. The screw is then passed over the guide pin and fixed into place. The guide pin is extracted and the slipped epiphysis is stabilized. The screws used in this study were approximately 90 to 100 mm in length.

The fixture (Figure 14) to induce acute SCFE allowed for even distribution of loading on the epiphysis with reusable fiberglass reinforced epoxy molds for repeatability in loading orientation. The two-piece epoxy molds were used



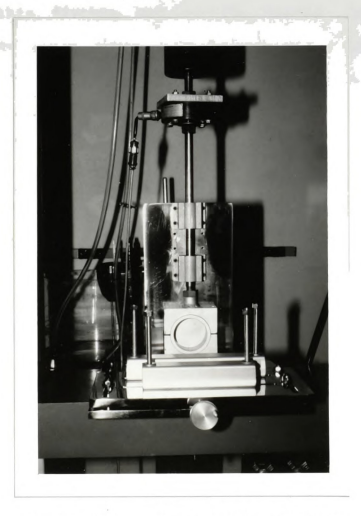


Figure 14. SCFE Inducing Fixture

to achieve a firm grip on the irregular geometry of the proximal femur. Preliminary experiments conducted at Wayne State University using steel clamps proved to be unreliable in preventing rotation and twisting of the femoral head and shaft during the AP displacement. The femoral head was also potted in this epoxy to eliminate stress concentrations caused by a steel loading ram⁷. A guide shaft with ball bearing pillow blocks was mounted to the back wall of the fixture to provide direct vertical loading on the femoral



head component.

With this fixture and potting system, complications such as greenstick bending, neck fractures, and epiphysis fractures noted by Chung⁷ et. al., were eliminated. The fixture was tested and provided a direct parallel shear on the bovine epiphyseal plates resulting in clean, repeatable slipped epiphyses. Any extraneous movement of the femoral shaft, neck or epiphysis was eliminated with this design as evidenced by monitoring tests with a video camera. Single and double screw fixation could then be compared biomechanically.

Ten pairs of fresh immature bovine femora were obtained from a local slaughter house. They were stripped of all soft tissue. Colleagues in orthopedic surgery inserted needles to locate the epiphyseal plate and radiographs were

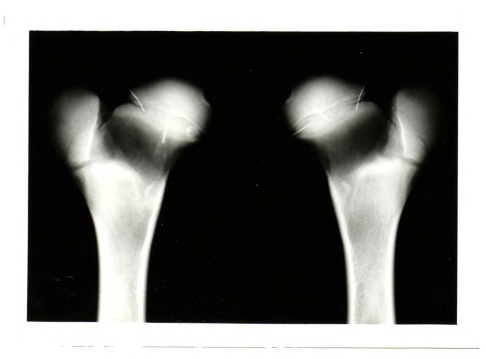


Figure 15. Bovine Femora Radiograph



taken to verify the precise location of the epiphyseal plate (Figure 15). The radiographs and femora, packed in ice, were sent by overnight express delivery to Michigan State University Department of Biomechanics, where they arrived approximately 18 hours later. They were sent two pairs at a time. When the femora arrived they were transected at the supracondylar level and the distal knee segments were discarded. Any excess soft tissue was removed and each femur was prepared for testing.

The proximal femora were potted in the quick-setting fiberglass resin up to the level of the physis (distal edge of epiphyseal plate), creating two-piece reusable molds (Figures 16,17). The radiographs and locating needles were observed during the potting process so as to align the plane of the epiphyseal plate vertically. The heads were then



Figure 16. Bovine Femur Mold





Figure 17. Two-Piece Mold



Figure 18. Potted Femoral Head



potted in a cup which will later be clamped in the fixture (Figure 18). The head was potted to the proximal edge of the epiphyseal plate making sure that it was not covered with the resin. The diameter of the epiphyseal plate was measured in the anteroposterior direction with calipers to an accuracy of $\pm 0.05\,$ mm (Figure 19). The specimens were kept moist with saline solution throughout testing.



Figure 19. Epiphyseal Plate Diameter

Each femur was placed in the custom-designed fixture mounted on an Instron model 1331 materials testing machine (Figures 20,21). A preload of 89N was applied and the femora were displaced in the anteroposterior direction, parallel to the epiphyseal plate, at a rate of one-third the diameter of the head per 10 seconds. The total displacement resembled a moderate, grade 1 slip of the epiphysis, or one-

e de la dec

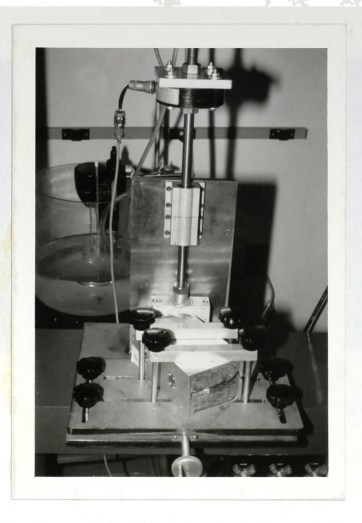


Figure 20. SCFE Specimen in Testing Machine

third of the diameter of the femoral head. Load-deformation data were recorded for each initial slip.

The femora were repacked in ice and sent back by overnight express to the orthopedic surgeon. Each slipped epiphysis was reduced and under fluoroscopy, and a single Asnis screw was placed into the central third of the epiphysis in one of each pair of femora. Two parallel screws were placed into the contralateral femur. Each pair served as its own control. Each screw was inserted





Figure 21. SCFE Specimen in Testing Machine

approximately four threads across the epiphyseal plate. Anteroposterior and lateral radiographs were taken to verify the slipped epiphyses and post-fixation pin position (Figure 22).

The femora and radiographs were shipped back to Michigan State University. When the internally fixed femora arrived the next day, they were retested in the original mold in a manner identical to the initial test. The specimens were sent back to the orthopedic surgeon after the second test for radiographs to document final pin position. The entire process was completed in approximately four days with the actual experimental testing completed in three days.

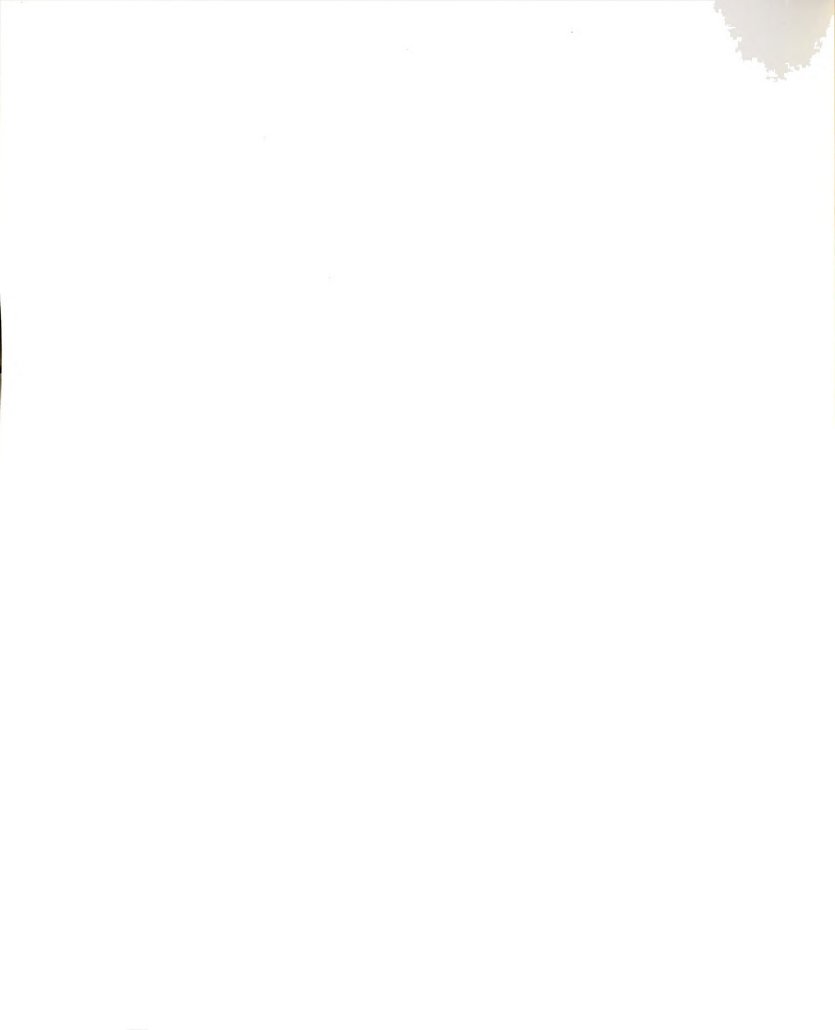




Figure 22. Post-Fixation Radiograph

For the initial slips, failure load, structural stiffness, average shear strength and strain energy (energy absorbed by the epiphyseal plate) were measured (Figure 30). Strain energy was computed as the area under the load-displacement curve to ultimate failure load. Thus, the strain energy may be thought of as a failure energy. For experiments on internally fixed specimens, strain energy was computed by integration to the displacement indicated at the point of initial epiphyseal plate fracture. The average shear strength was calculated as the failure load divided by the estimated circular cross-sectional area of the epiphyseal plate. This calculation allowed a comparison to the data from Chung⁷. A statistical analysis (paired



Students t-test) of data comparing left versus right femora was also examined to verify the experimental method and reproducibility of the bovine SCFE model. Experimental data was analyzed (paired Students t-test) for post-fixation tests to compare single and double screw fixation.

B. Finite Element Analysis

A simple mechanics analysis of the SCFE internal fixation problem may be given by a simply supported beam with an overhanging \log^{41} (Figure 23).

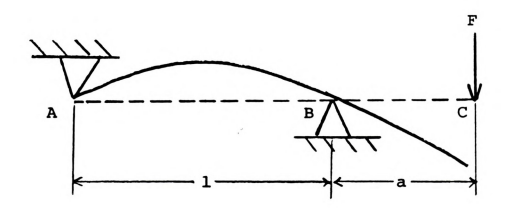


Figure 23. Simply Supported Beam

The deflection at the end of the beam (screw) is given by

$$y = \frac{Fa^2}{3EI}(1+a) \tag{15}$$

where

F = applied force

E = elastic modulus

I = moment of inertia



$$= \frac{\pi}{(d_0^4 - d_1^4)}$$
 (16)

and $\mathbf{d_0}$ and $\mathbf{d_i}$ are outer and inner diameters respectively for a round, hollow beam. Yet, the problem of internal fixation of SCFE is probably more complicated than the simple beam analysis given above, since the screw is surrounded by bone. The internally fixed epiphysis model is actually one of a beam-like support structure surrounded by a foundation of bone with its own elastic modulus and Poisson's ratio. To more fully describe these two interfacing materials, a finite element analysis was employed.

Relevant finite element studies have examined plated long bones 3 , 40 and others have examined femoral head load changes occurring with infarction and normal growth 5 . Many other studies have analyzed the design of prosthetic hips, the implant of prosthetic hips and the interfaces between bone and cement 39 . No study, to date, has examined the internal fixation of SCFE with single and double screws.

The finite element models (Appendix B) were developed to estimate the effect of single and double screw fixation on structural stiffness of slipped capital femoral epiphysis. The models provided a method to compare the structural responses of the internally fixed epiphysis. A parametric analysis was also conducted to examine a possible optimization of single screw fixation.

The single screw finite element model consisted of 175 nodes with 120 3-D isoparametric solid elements (Figure 24).



The elements are defined by eight nodal points each having translations in the nodal x, y, and z directions. Prism shaped elements are defined by duplicating two nodes. The element has plastic, creep, swelling, stress stiffening and large rotation capabilities. A generalized plane strain option is also available. The solid screw was modeled as a series of elements in the center of a cylindrical shaped model of bone 50 mm in diameter. The diameter was based on the observed average bovine epiphyseal plate. A 1 mm gap simulated the separated physis and no interfaces were

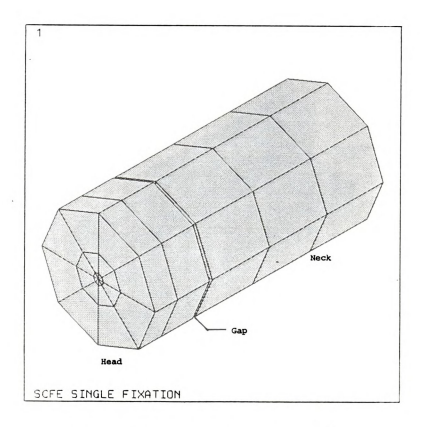
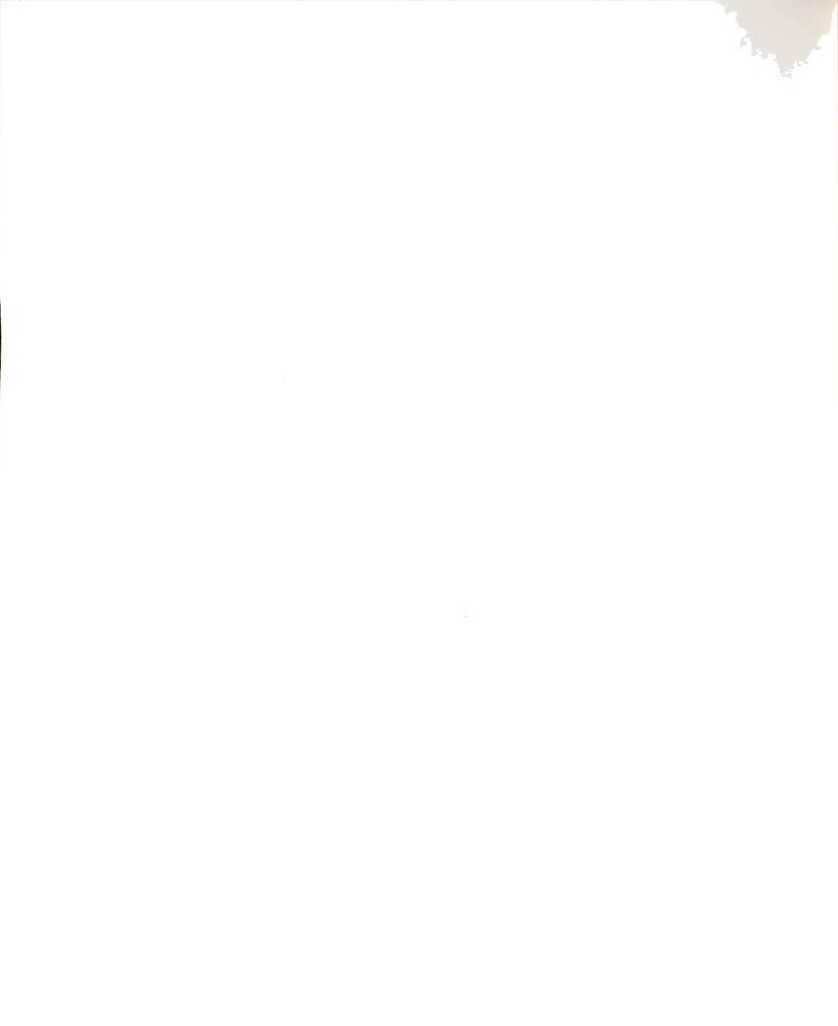


Figure 24. Single Screw FEM

assumed in this region. In experimental testing, there are shear and frictional effects in this region which are



unknown and may increase the structural stiffness of the model. The 90 mm screw passed through the bone cylinder, across the gap and terminated 10 mm from the end of the femoral head portion. There was also no interface assumed between screw and bone as both were modeled with the same type of elements, directly connected, with different moduli and Poisson's ratio (Figure 25). For presentation reasons, symmetry was not exploited.

An elastic modulus of 780 MPa was used for the "bone" elements, and a Poisson's ratio of 0.14 was selected 31. Elastic moduli ranging from 57 MPa to 780 MPa have been

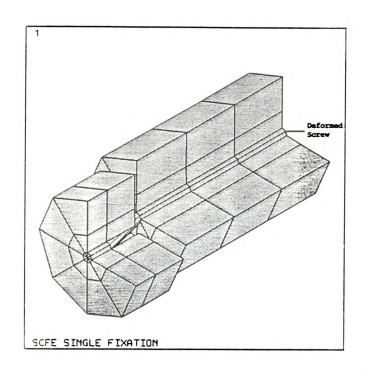
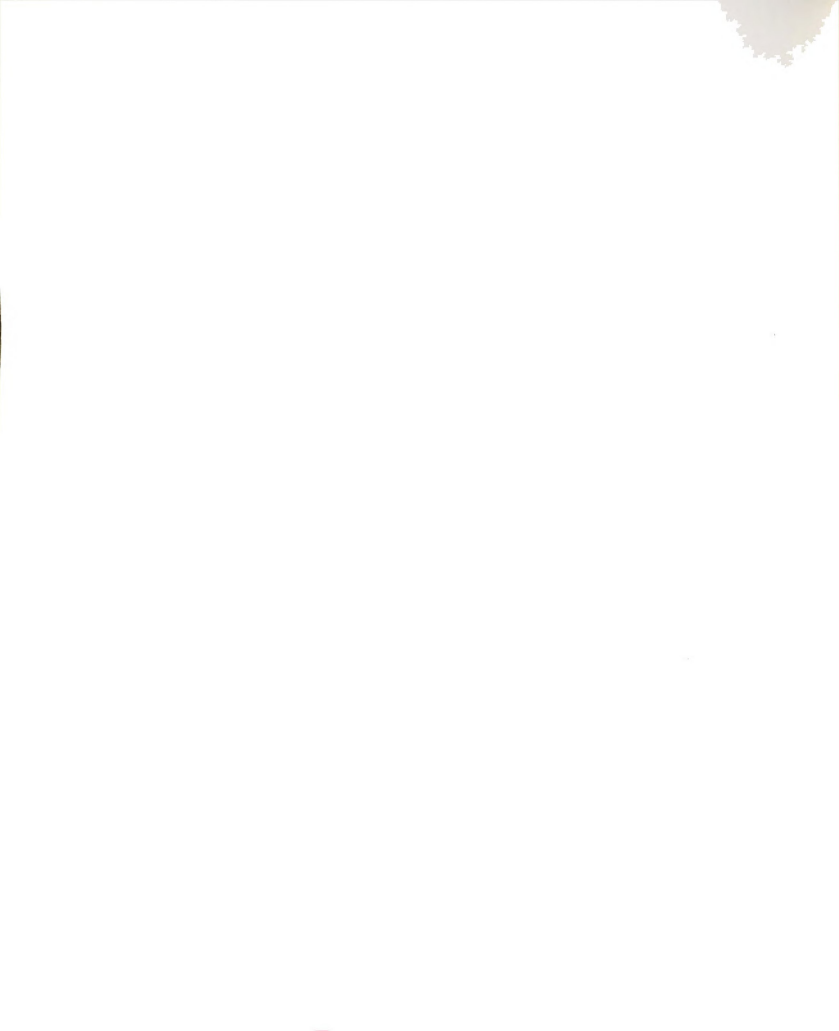


Figure 25. Sectioned Single Screw FEM

reported 31 . The highest mean modulus of elasticity was found in the femoral neck region (Table 3). In the experimental study, the screw(s) were noticed to have the



most mechanical effect on the bone in the neck region. Microstructural bone failure and widening of the screw hole was observed. Therefore, the femoral neck modulus was used in this finite element study.

Table 3. Reported Bone Moduli 31

	Specimen	Modulus (MPa)			
Human	Femoral Head	57 (anteroposterior)			
Human	Femoral Head	87 (direction of neck)		
Human	Femoral Head	581	17		
Femor	al Neck	780	41		
Human	Femoral Head	344	27.6		

The double screw model (Figure 26) consisted of 341 nodes with 260 3-D isoparametric solid elements. The screws were oriented about the center of the cylinder parallel to

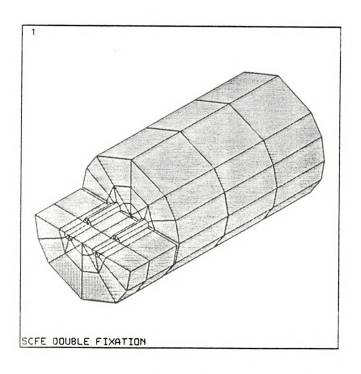


Figure 26. Double Screw FEM



each other to replicate experimental double screw fixation. All material properties and screw dimensions were similar to the single screw model.

An elastic modulus of 190 GPa and Poisson's ratio of 0.305 were used for the stainless steel (316L) Asnis screw(s) 27 . The screws were modeled as solid cylinders without threads. The Asnis screw, described earlier, has a cannulation of 1.6 mm with a shank diameter of 4.5 mm and thread diameter of 6.4 mm.

To simulate the experiments, the boundary conditions for the FEM were such that a 6 mm vertical displacement was set on the upper nodes of the femoral head elements. The lower nodes were left free to displace. Displacements for all other external nodes in the neck region were set to zero, simulating the stabilized proximal femur in its mold (Figure 27). The average displacement to failure of the epiphyseal plate in experimental tests was approximately 6 mm, therefore, this value was used in the FEM analysis.

Reaction forces on the upper nodes were summed and divided by 6 mm to calculate the structural stiffness of each model. A parametric analysis was undertaken to analyze the effects of changing the FEM single screw diameter from $4.5 \, \mathrm{mm}$ to $7.5 \, \mathrm{mm}$.



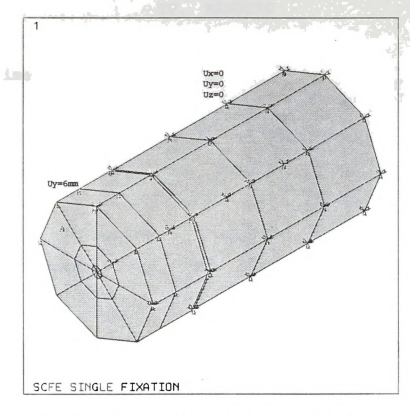


Figure 27. FEM Boundary Conditions



A. Experimental

In all twenty femora, acute anteroposterior slips of the femoral epiphyses were created (Salter type I). No femoral neck fractures were seen, nor was bending or twisting of the specimens within the fixture noted during the displacement of the femoral head (Figure 28).



Figure 28. Bovine Slipped Epiphysis in Fixture

Examination of the epiphyseal plate revealed a complex geometrical structure consisting of many mamillary processes and an irregular surface area (Figure 29). A typical load-deformation curve for the initial slip is shown in Figure 30. Failure load was defined at the point of epiphyseal





Figure 29. Epiphyseal Plate

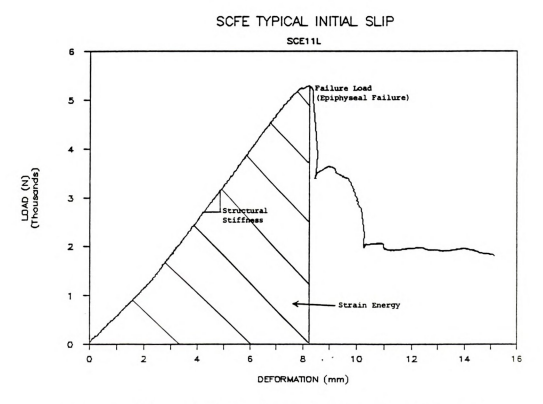


Figure 30. Typical Load-Deformation Curve



plate failure. This was represented by an abrupt drop in load.

Structural stiffness was determined by linear regression of data to the point of epiphyseal failure. Since the failure loads were above the range of normal physiological loading on the hip, structural stiffness was also calculated by regression to the point of maximum in vivo loading (1000 N). This value was approximated by using Equation 11 from Litchman and $Duffy^{23}$ which gives a calculation for the anteroposterior vector, $\mathbf{R}_{_{\mathbf{U}}}$, representing these experiments. From Paul's 36 data (by interpolation), the total reaction force, R, on the femoral head during fast walking is 6.8 times body weight. This was found to occur at 7% of the gait cycle immediately after heel strike with $\phi_1\!=\!21^\circ$ and $\phi_2=\!12^\circ$ (Figure 12). For a thirteen year old 95th percentile overweight male and female the average $weight^{16}$ is 649 N. Thus, a value of 918 N is calculated for the anteroposterior loading on an overwieght individual's hip during fast walking. This value is rounded to 1000 N in attempt to cover a wider range of in vivo loading on the hip (i.e. running, jumping, etc.).

In analyzing test data (Appendix A) from left and right specimens for the initial slip, no statistical difference (p>0.05) in stiffness, average shear and strain energy was found (Table 4). There was a high range of failure load observed (2,800-8,200 N) and it was found to be greater in left specimens (p<0.05) for this particular study. There was no significant correlation between failure load and



epiphyseal diameter (p>0.05, r=0.03, Figure 31). The computed average shear stress was found to decrease with larger diameter specimens (p<0.05, r=0.47). When the high failure load specimens were removed from this analysis, no significant correlation between diameter and shear strength was observed (p>0.05, r=0.23, Figure 32).

Table 4. Intact Epiphyseal Plate Structural Responses

	ו דייים דו	PEMITO	DICUT	PEMIID	IALL SPECIMENS			
	DEFI	EMOR	KIGHI	FEMOR	IALL SPECIMENS			
FAILURE LOAD (N)	14,947	1,250	4,501	± 1,064	4724 ± 1182			
STIFFNESS (N/mm)	800	198	728	± 180	764 ± 193			
AVG SHEAR (MPa)	2.49	0.85	2.26	± 0.65	2.37 ± 0.76			
STRAIN ENERGY (J)	18 ±	11	16	± 6	17 ± 9			
(mean ± s.d.)								

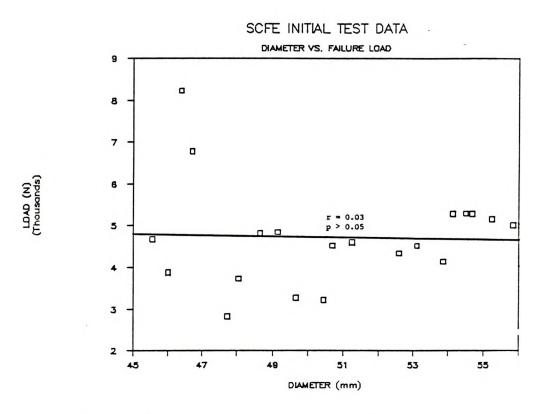
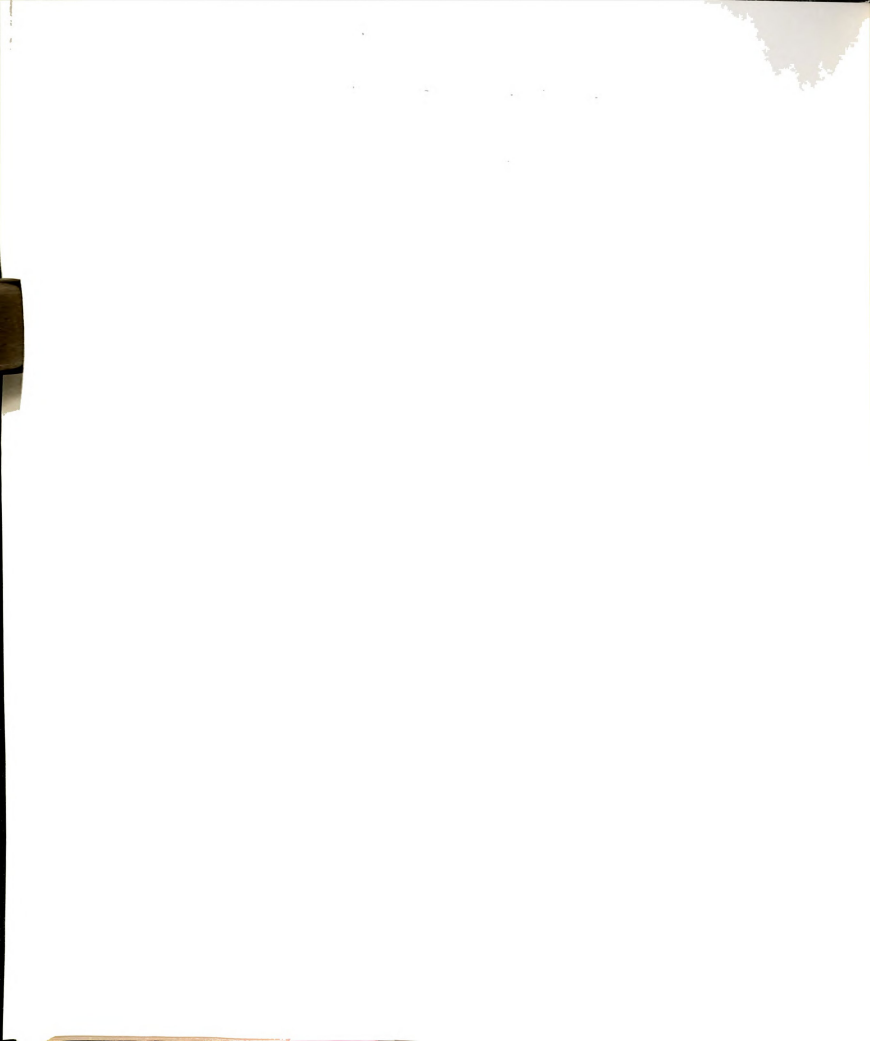


Figure 31. Diameter Versus Failure Load



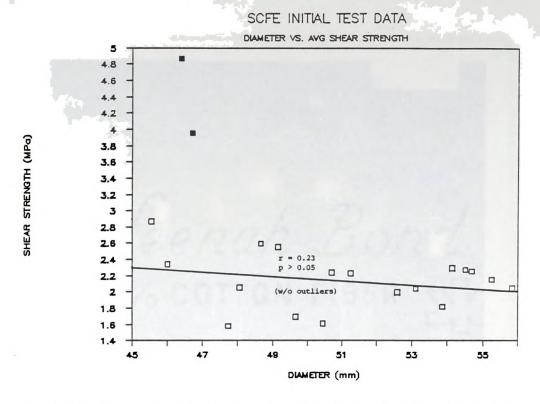
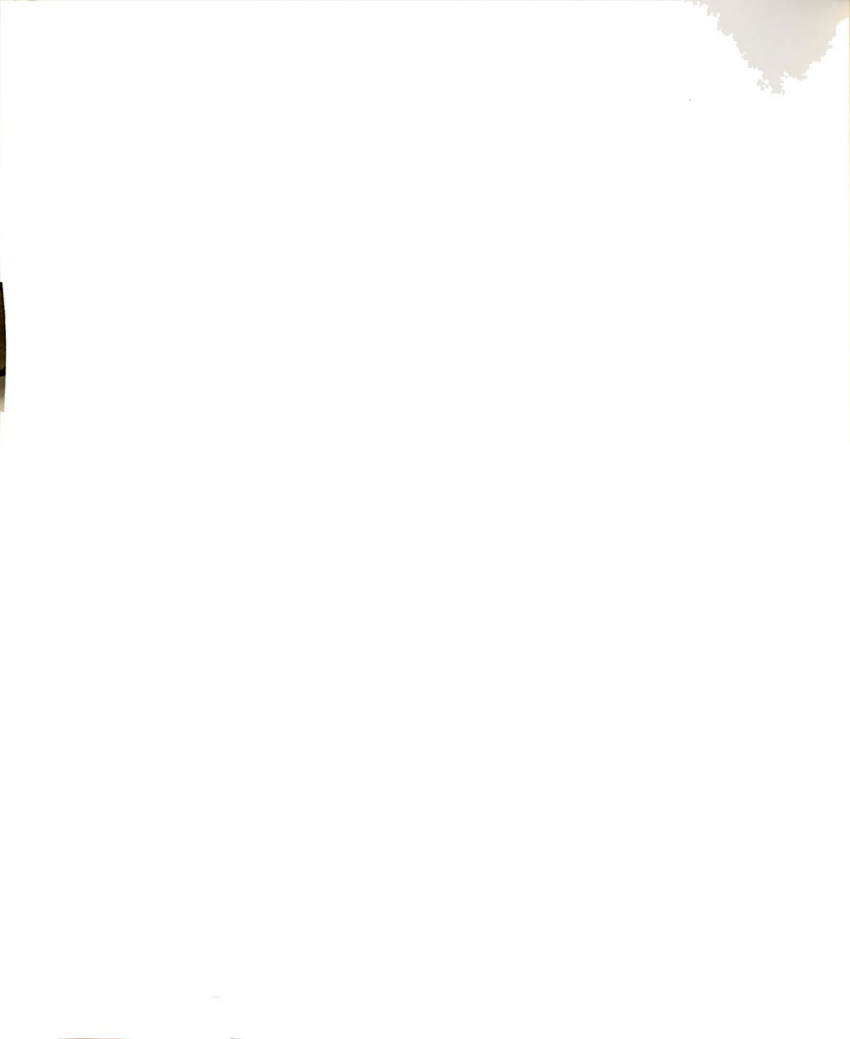


Figure 32. Diameter Versus Average Shear Strength



Figure 33. Highly Calcified Specimen



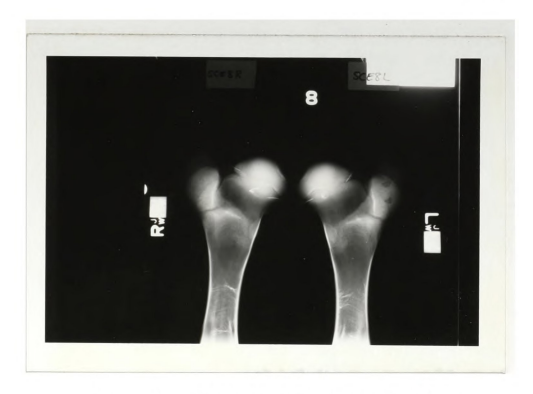


Figure 34. Normally Calcified Specimen

The high failure load specimens, SCE-12L and SCE-12R, were examined by radiograph and were found to be more calcified than others in the study. Figure 33 reveals a thick walled femoral shaft and narrow epiphyseal plate region, while Figure 34 shows a normal, less calcified specimen.

Internal fixation radiographs revealed that the single screw pivoted with slight bending during testing, while the double screws tended to pivot only (Figure 35). Thus, examination of post-fixation load-deformation data did not indicate a clear sign of failure, such as an abrupt drop-off in load noted in the initial tests (Figure 36). Therefore, we used a "gross" structural stiffness or resistance to slip

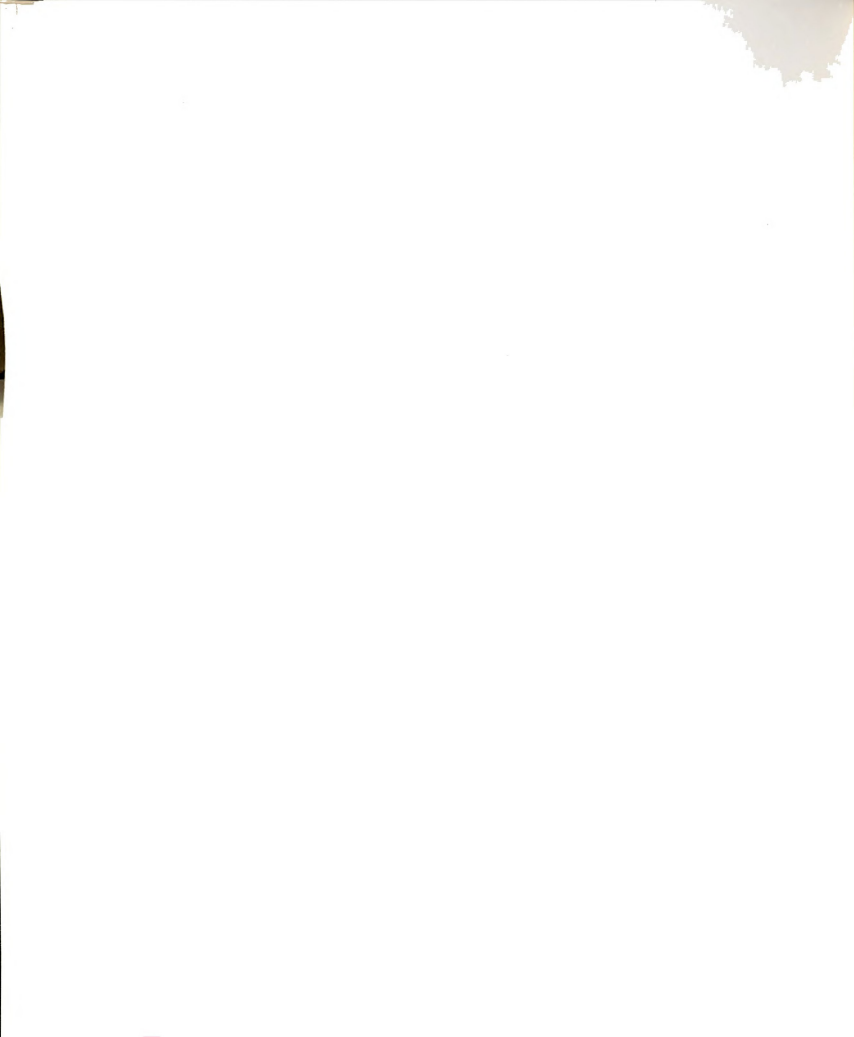




Figure 35. Internal Fixation Radiograph

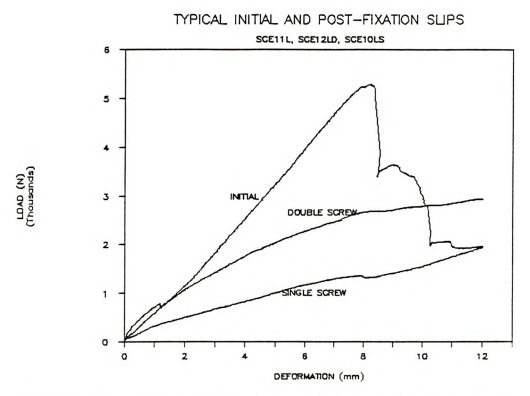


Figure 36. Typical Initial and Fixation Responses



in a deformation of one-third the epiphyseal diameter to compare single and double fixation responses. A significant decrease in gross structural stiffness (k) was found in post-fixation tests (Figure 37). Using each pair as its own control, the average ratio of stiffness for double to

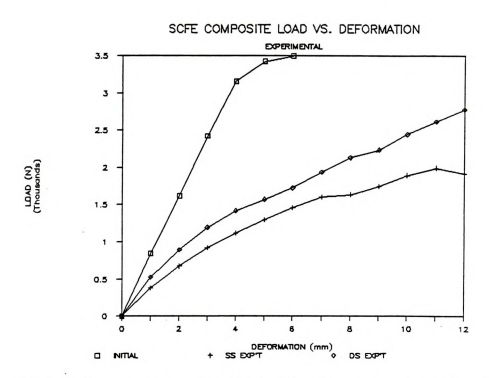


Figure 37. Average Initial and Fixation Responses

single screw fixation (k_d/k_s) was found to yield only a 33% increase in resistance to slip with two screws (p<0.05). When examining the "in vivo" structural stiffness, no significant difference (p>0.05) was found between single and double fixation (Table 5).



B. Finite Element Analysis

Using the simple beam analysis (Equation 15), a reaction force of 3,400 N was calculated for a 6mm vertical deflection yielding a stiffness of 567 N/mm. This analysis assumed a solid, round beam. The finite element models indicated structural responses more similar to that of the experimental data. Structural stiffnesses of 195 N/mm and 284 N/mm were found for single and double screw fixation, respectively. The finite element models yielded a 45% increase in structural stiffness when double screw fixation was used. Table 5 and Figure 38 indicate that experimental and finite element data compare favorably. In examining the

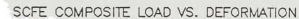
Table 5. Experimental and FEM Stiffness Data

FIXATION	EXP'T gross k (N/mm)	EXP'T in vivo k (N/mm)	FEA
SINGLE	149 ± 40	334 ± 214	195
DOUBLE	193 ± 39	431 ± 193	284
k_d/k_s	1.33 ± 0.28 (avg ratio)		

epiphyseal plate region, higher average stresses were found in the double screw model and these stresses occurred over a greater area (Figures 39, 40).

A number of parametric studies were also conducted using the finite element models. When the outer diameter of the bone cylinder was doubled in both models, the double screw was found to be only 41% stiffer than the single





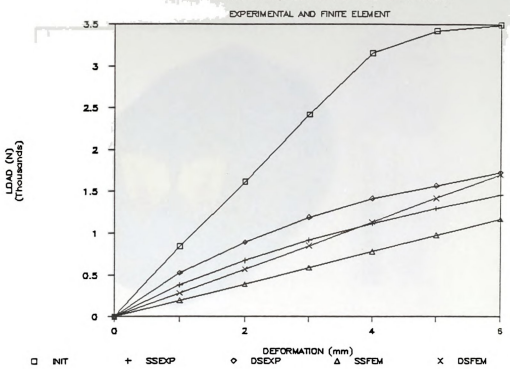


Figure 38. Experimental and FEM Responses

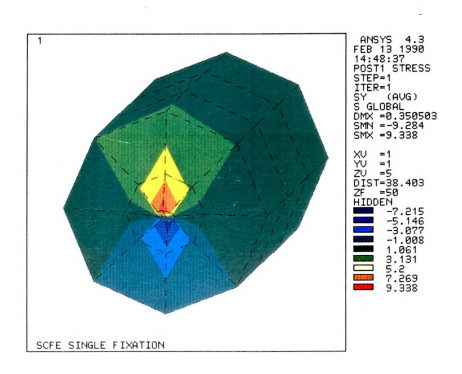


Figure 39. FEM Single Screw Stresses



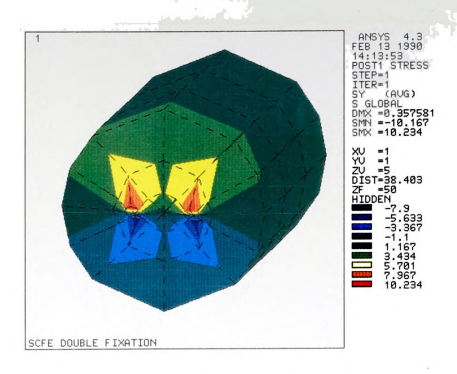


Figure 40. FEM Double Screw Stresses

screw. When the modulus of bone was changed to equal the modulus of the screw and the models were run under the same conditions, the double screw yielded a 45% increase in stiffness over the single screw. Results of the above parametric studies were similar to the initial model results.

Another study was undertaken to determine the effects of increasing the single screw diameter. When the theoretical diameter was increased from 4.5 mm to 5.5 mm, the structural stiffness of the model compared to experimental data for double screw fixation (Figure 41). By increasing the diameter of the model to 7.5 mm, the structural stiffness approached that of the experimental



data for the intact epiphyseal plate.

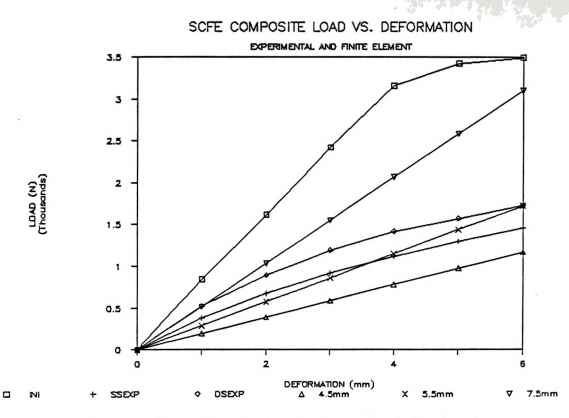


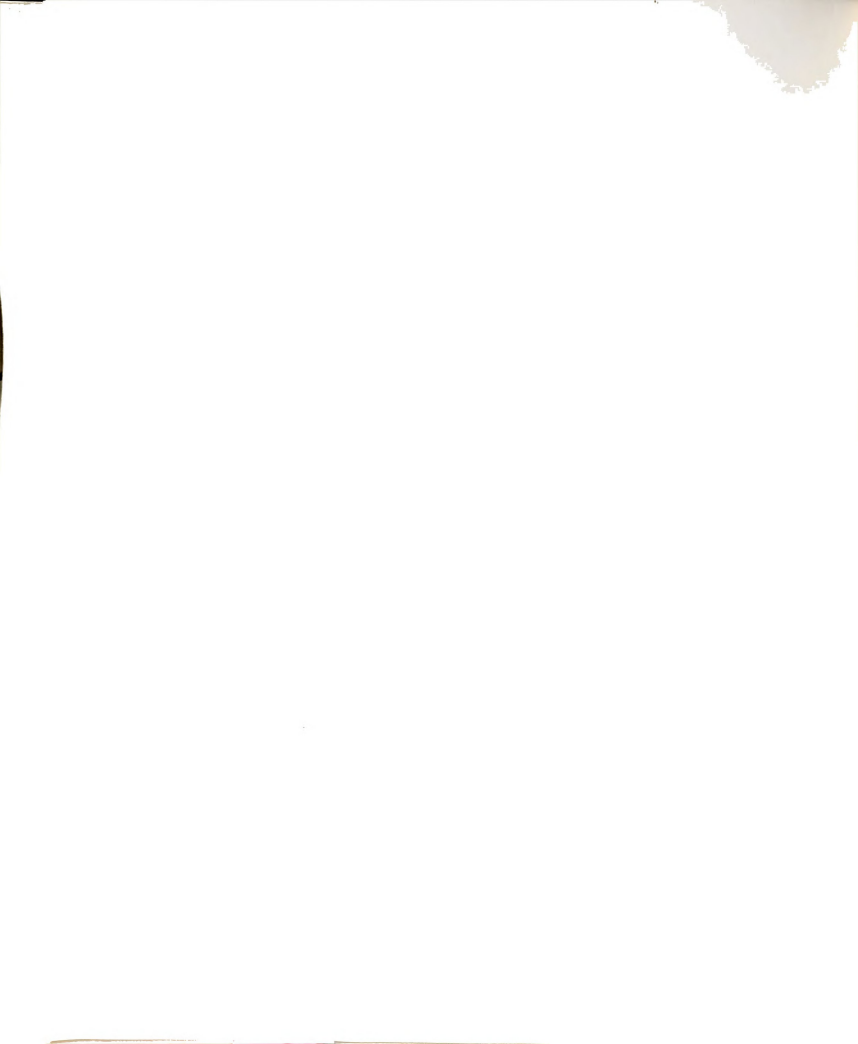
Figure 41. Single Screw FEM Optimization



A. Experimental

The experimental data represents important biomechanical properties for fixed epiphyseal response over a direct shear of one-third the epiphyseal diameter in the anteroposterior direction. The actual physiologic loading on the hip has components in the anteroposterior and medial lateral directions running downward relative to the femoral axis (Figures 11,12). This study ignored the normal component to the epiphyseal plate. The normal component is likely to increase the resistance to shear of the epiphyseal plate by increasing frictional forces within this complex surface area (Figure 29). These frictional forces may be non-linear in nature.

A reproducible bovine femora SCFE model was developed. The SCFE fixture repeatedly slipped the epiphyseal plates without complications, unlike the fixture used by ${\rm Chung}^7$. No statistical differences were found in structural stiffness, average shear and strain energy between left and right specimens. There was, however, a statistical difference in failure load between left and right specimens. A large range of failure loads was found for the initial slips. The failure load was found to be independent of diameter (p>0.05), but the average shear stress was found to decrease with increasing diameter (p<0.05). It was initially thought that diameter correlates with age and that



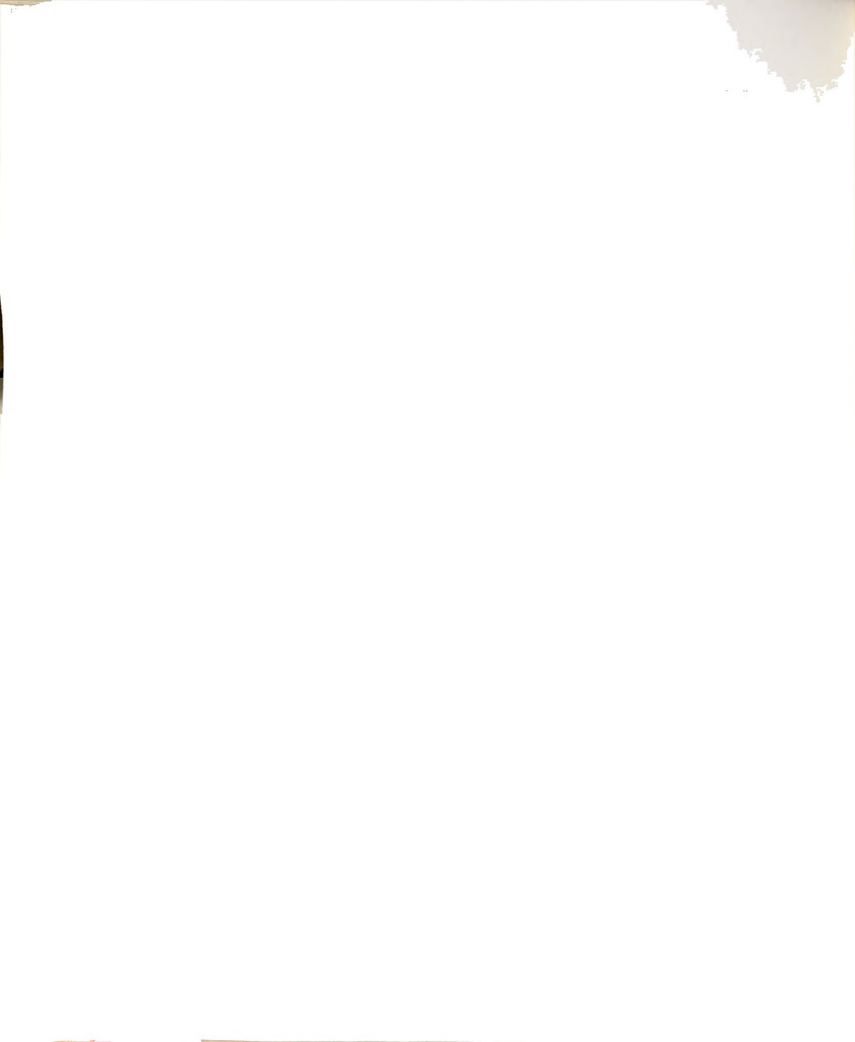
the shear stress must increase with increasing diameter, as ${\sf Chung}^7$ (Equation 14) has shown in humans.

Differences in age, feeding programs, or specimen breeds may cause variability in the data. In fact, the high failure load specimens (SCE12L and SCE12R, Figure 31) had relatively smaller epiphyseal plate diameters (46.38 and 46.7 mm) which suggests that they may be from a smaller breed of calf, which is more mature. When these specimens were removed from the average shear strength data, no significant trend with diameter was observed (Figure 32).

The wide range of failure load observations may also be due to slight variances in the orientation of loading on the plate caused by inconsistent potting technique or alterations in mounting the specimens on the fixture. If the epiphyseal plate was not parallel with the loading direction, a normal component would produce increased frictional forces due to the irregular geometry of the epiphyseal plate.

An average shear strength of 2.37 ± 0.76 MPa was found for bovine calf epiphyseal plates. Chung found a shear strength of 1.16 MPa in a 13 year old human femoral epiphyseal plate and using Equation 14, a shear strength of 1.35 MPa was calculated for a 13 year old person. Given experimental error, the shear strength of the human and bovine proximal femoral epiphyseal plate is comparable.

The average ratio of gross stiffness for double to single screw fixation yielded only a 33% increase with double screws (p<0.05). $Kruger^{21}$ found similar results with

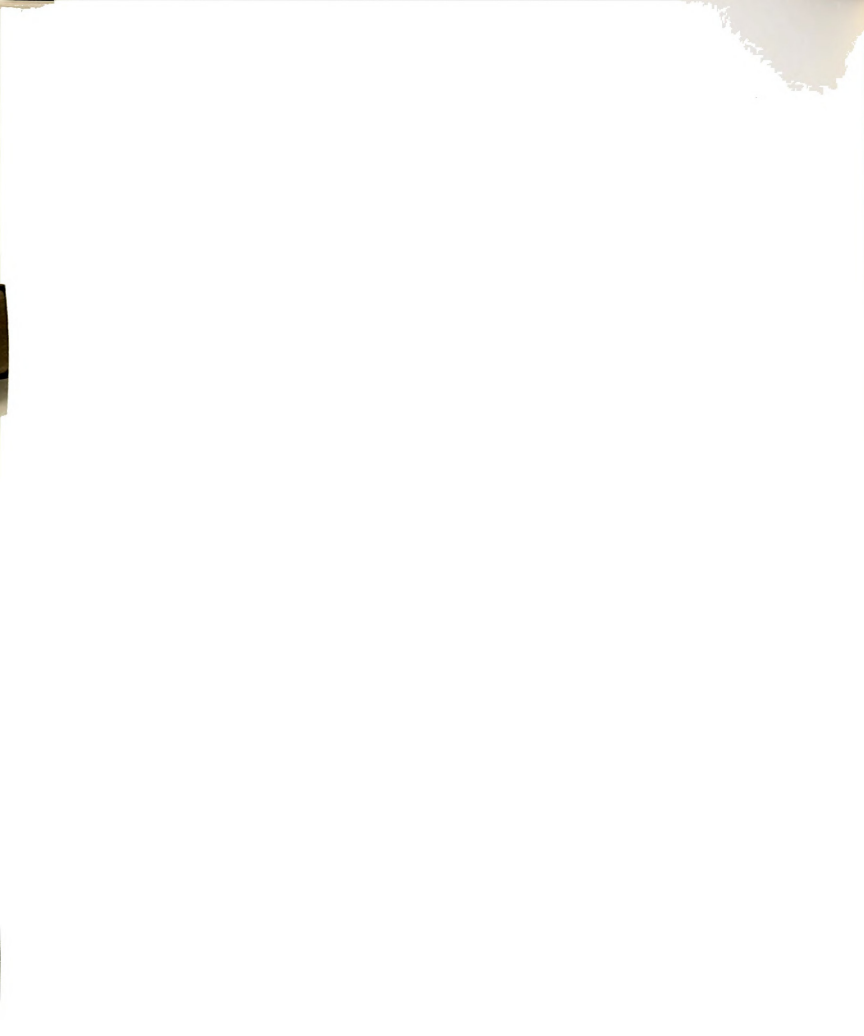


a 22% increase in stiffness with double Steinmann pin fixation over single pin fixation. When "in vivo" structural stiffness was examined, no significant difference was found between single and double screw fixation. The "in vivo" data may be related to the clinical situation. These data suggest that an overweight adolescent may begin limited weight bearing activities on the slipped epiphysis after internal fixation with a single Asnis screw as soon as he would with double screw fixation.

B. Finite Element Analysis

The reaction force and resulting stiffness calculated in the simple beam analysis, using a 6mm vertical displacement, were over double those of finite element results. The displacement in experimental testing and finite element models is applied to the perimeter of the femoral head and not directly to the screw, as was done in our simple beam analysis. Therefore, to input the proper deflection into the beam equation, the displacement at the end of the screw in the finite element model was examined. A displacement of 5.9mm was found. If this displacement is applied to the simple beam analysis, reaction load and stiffness are only reduced by 1.7%. The results of the beam equation remain uncomparable to finite element analysis results.

The linear finite element models yielded similar structural results as compared to experimental data (Figure

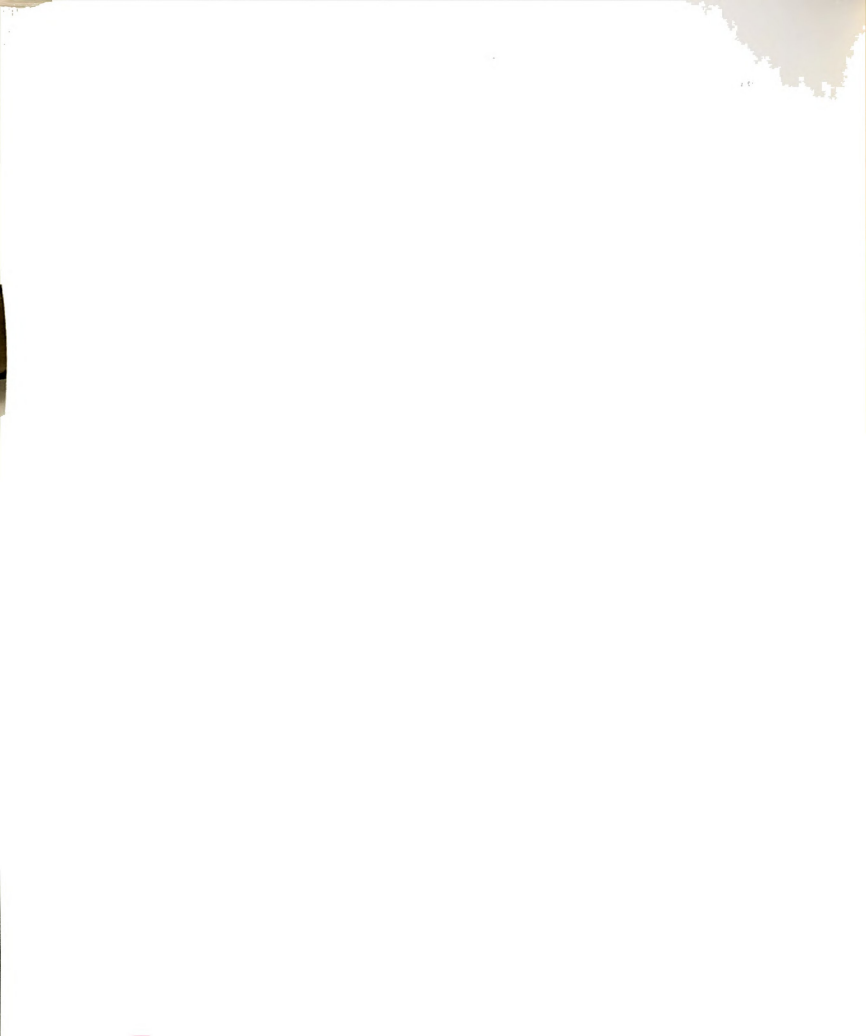


38). A 45% increase in structural stiffness was found for double screw fixation over single screw fixation. The results again indicate that structural stiffness is not proportional to the number of screws used to fix the slipped epiphysis. The FEM results were based on a reported human, femoral neck bone modulus of 780 MPa.

In an attempt to explain the disproportional increase in structural stiffness (only 45% increase in stiffness with two screws), stress plots of the epiphyseal plate region were examined. The plots revealed that slightly higher stresses were present within the face of the epiphyseal plate in the double screw model and these stresses occurred over a larger area (Figures 39,40). The higher observed stresses may cause increased bone deformation around the two screws relative to the single screw. Thus, there is increased support with addition of another screw, but this was thought to be offset by increased stress, and relatively greater strains within the bone surrounding the screw.

In an attempt to further explain this phenomenon, the diameters of both single and double screw models were doubled to 100 mm. This was done in attempt to reduce the stress concentration around the double screw model and therefore, increase the structural stiffness. Instead a slight decrease in the ratio of double to single screw stiffness was observed (41%). Thus, no explanation was available as to why there was only a 45% increase in stiffness with two screws.

Another study was conducted to help determine whether



the disproportional increase in structural stiffness with two versus one screw was simply due to the screws being in series, rather than parallel, to the bone. The modulus of the bone was made equal to the modulus of the screw, but again a 45% increase in double screw stiffness over single screw was found. This suggested that the results were not just those of the screw and bone being simply in series.

The remaining parametric study revealed that increasing the diameter of the single screw to 5.5 mm will cause the structural stiffness to be comparable to that of the experimental double screw stiffness. This amounts to only a 49% increase in cross-sectional area over the 4.5 mm diameter screw. By further increasing the diameter of the single screw to 7.5 mm, the structural stiffness of the FEM approaches that of the experimental intact epiphyseal plate (Figure 41).

Obviously, by increasing the diameter of the fixator screw, more beneficial biomechanical results are obtained, but the amount of cross-sectional area entering the femoral neck and head has to be limited for biological reasons. As described earlier, the femoral head and neck has a rich vascular supply and the more material entering this environment, the more possibility of interruption of blood supply and resulting necrosis. If necrosis does occur, then the bone surrounding the screw will be weakened and the fixation on the slipped epiphysis will be lost. Studies have shown that as the number of screws used to fix the slipped epiphysis increase, so do the number and severity of



complications such as necrosis and chondrolysis 42. Therefore, by optimizing single screw fixation and limiting invasion of bone by the screw, a more biomechanically and biologically favorable fixation of SCFE might be obtained.

Although, the finite element analysis provides a method to analyze SCFE internal fixation and optimize single screw fixation, there are limitations to the models in this study. The finite element models are only crude geometrical representations of the internally fixed proximal femur. The femoral head is actually spherical in shape and the femoral neck has a smaller, non-constant diameter. There is also no representation of the epiphyseal plate in these models, only a 1 mm gap. The epiphyseal plate (Figure 29), as explained earlier, is a complex geometrical structure that may provide additional shear resistance. Three dimensional interface elements, such as those in ANSYS may provide a method to represent the epiphyseal plate with non-linear frictional forces.

Ideally, the mesh in the finite element model should be refined by increasing the number of elements and comparing results (displacements, stresses) to initial model results. If there is no significant difference in the results of the two meshes, they are converged on a solution. The elements, particularly within the epiphyseal plate region, could be refined. This is the region where bending of the screw(s) takes place in the FEM. As discussed earlier, the screw(s) were experimentally observed to pivot with slight bending away from the plate within the femoral



neck (Figure 35). By refining the models, a better representation of the experimental results should be obtained. Also, a constant human femoral neck modulus was used in the finite element models. The modulus actually varies from head to neck with a wide range of moduli reported 31.

Another limitation of the finite element study may be found in the modeling of the screws. The screws were modeled as solid cylinders without threads. The threads comprise only the last 20 mm of the screw projecting away from the shank. They would seem to provide little support in a bending analysis, although they may prevent the femoral head from slipping off the shank under large deformations. Neglecting the cannulation, has little effect on stiffness since the moment of inertia (Equation 16) changes from 19.81 mm 4 for a hollow screw to 20.13 mm 4 for a solid screw.

Further improved finite element models could be utilized to examine single and double screw fixation and together with experimental testing, optimize single screw fixation of SCFE. Future studies should also include a more in vivo type of loading on the epiphysis. One that could include the frictional forces within the epiphyseal plate. Beaupre³, et.al., used sliding frictional interfaces in a plated long bone to examine the effects of screw tightness. Schwartz⁴⁰ also used sliding interfaces in another plated bone study. Single and double screw fixation could then be compared. Many different types of cyclic loading could be applied (i.e. walking, running, jumping) to evaluate

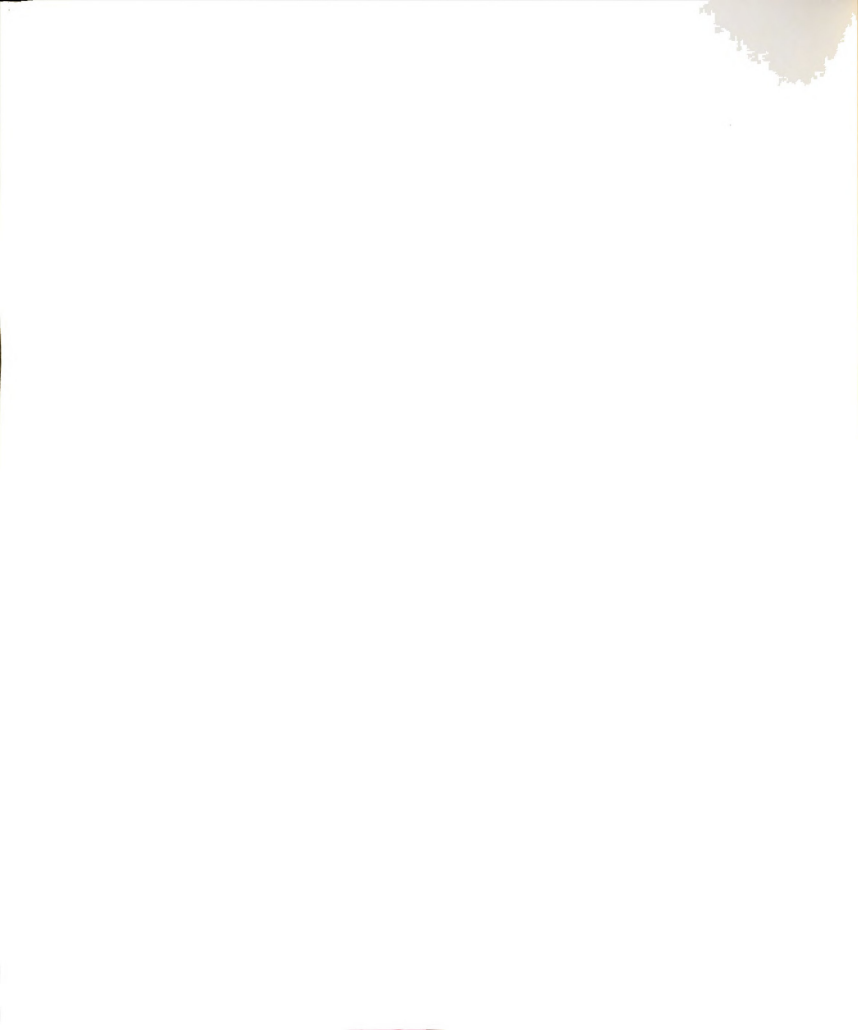


internal fixation. This would lead to more direct conclusions as to the type of weight bearing the patient can undergo after internal fixation of SCFE.

A live animal model, possibly bovine calf, could be developed in which SCFE is induced. Standard single and double screw fixation could be examined biologically and biomechanically. The slipped epiphysis could also be fixed with an optimized single screw (possibly through finite element analysis) and examined over a time history to include bone remodeling and biological factors (observations of necrosis or chondrolysis).

In conclusion, the experimental "in vivo" stiffness data revealed no significant difference between single and double screw fixation of SCFE. Only a 33% increase (p<0.05) in gross stiffness was found for double screw as compared to single screw fixation. The actual physiological load orientation on the hip serves to reduce the shear stress on the epiphyseal plate and thus, reduce the load bearing activity of a single screw. Given this fact, single screw fixation seems even more biomechanically favorable. Considering the available clinical data on single screw fixation and reported complications associated with multiple screw fixation, a single screw is recommended by this study for the internal fixation of SCFE.

While further refinement and interface elements may yet be needed in the gap region, results of the finite element model indicate that a minimal increase in the diameter of a single screw fixator will result in a significant increase



in the structural stiffness of the internally fixed SCFE. In the future, the use of an optimized single screw fixator could reduce the reported surgical complications associated with multiple screw fixation while increasing stability of internally fixed Slipped Capital Femoral Epiphysis.



APPENDIX A



APPENDIX A

Table 6. SCFE Initial Test Data

SPEC	DIA mm	CSA mm ²	FAIL LD N	DEF mm	SHEAI MPa	R k gro N/mm	k phy N/mm	ST ENG J
6L 6R 7L 7R 8L 9R 10L 11R 12L 13R 14L 14L 15R	45.55 46.00 55.85 55.25 49.65 50.70 53.10 53.10 53.50 54.68 54.50 46.38 46.30 49.14 48.05 47.73 54.13 53.88	1629.5 1661.9 2449.8 2397.5 1936.1 1999.0 2018.9 2214.5 2214.5 2171.4 2348.3 2332.8 1689.5 1712.9 1836.3 1789.3 2201.3 2277.5	4677.0 3839.3 5015.2 5157.6 3279.7 3221.8 4601.3 4525.7 4521.2 4343.2 4343.2 4341.1 5300.0 8223.6 6777.4 4841.6 4843.8 3729.1 823.8 3729.1 823.6 6775.6	9.14 10.73 9.64 5.87 5.59 5.05 4.98 4.33 4.68 9.41 5.59 9.41 7.43 6.89 6.21 4.70 5.43 4.88	2.87 2.34 2.05 2.15 1.69 1.223 2.24 2.04 2.00 2.25 2.27 4.87 3.965 2.60 2.06 1.58 2.38 2.38	563.9 378.8 520.9 866.5 626.6 663.1 742.9 1078.6 922.4 680.0 927.0 832.0 846.9 775.3 829.5 634.3 1137.9	1559.4 1119.5 739.4 351.8 666.0	17.6 21.1 30.9 14.8 10.9 12.4 15.2 11.9 21.5 143.9 21.5 15.6 8.2 8.8 12.6
MAX	55.85	2449.8	8223.6	10.73	4.87	1137.9	1559.4	43.9
MIN	45.55	1629.5	2825.8	4.33	1.58	378.8	236.8	8.2
VAR	10.79	68423	1397149	3.69	0.58	37115	161555	74.2
DEV	3.28	261.6	1182.0	1.92	0.76	192.7	401.9	8.6
AVG	50.71	2028.1	4723.7	6.67	2.37	764.0	811.8	17.0

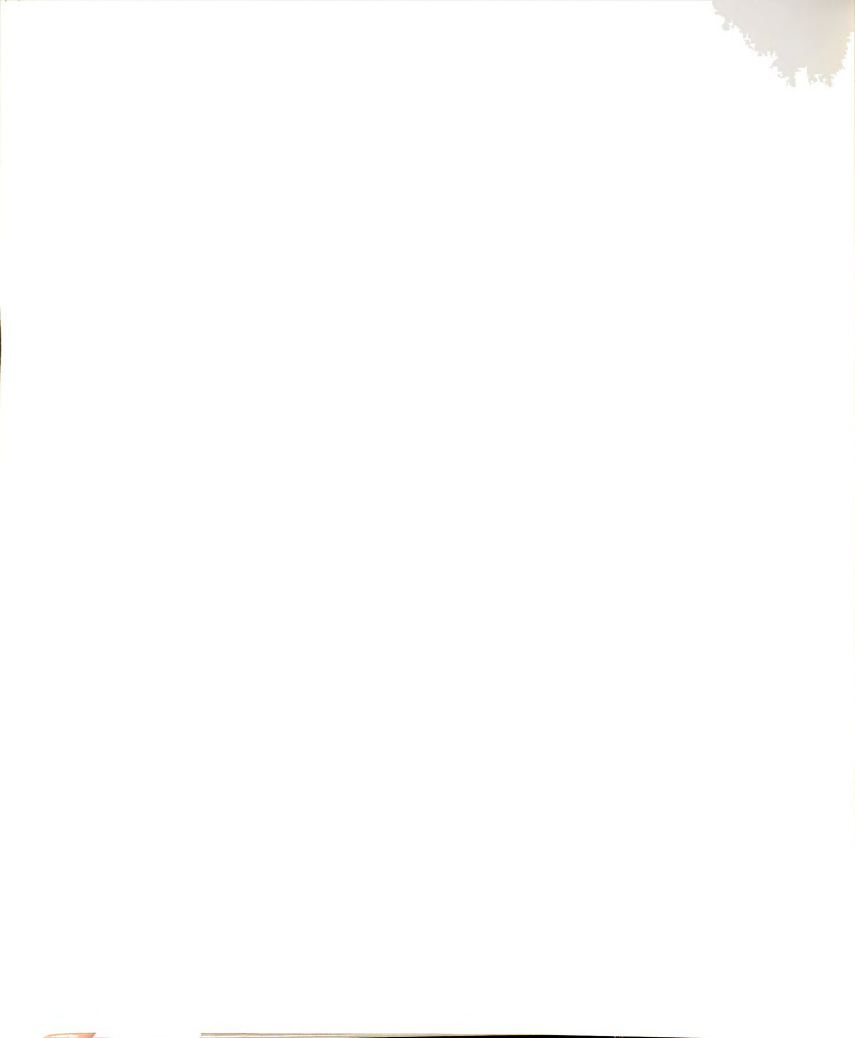


Table 7. Single Fixation Test Data

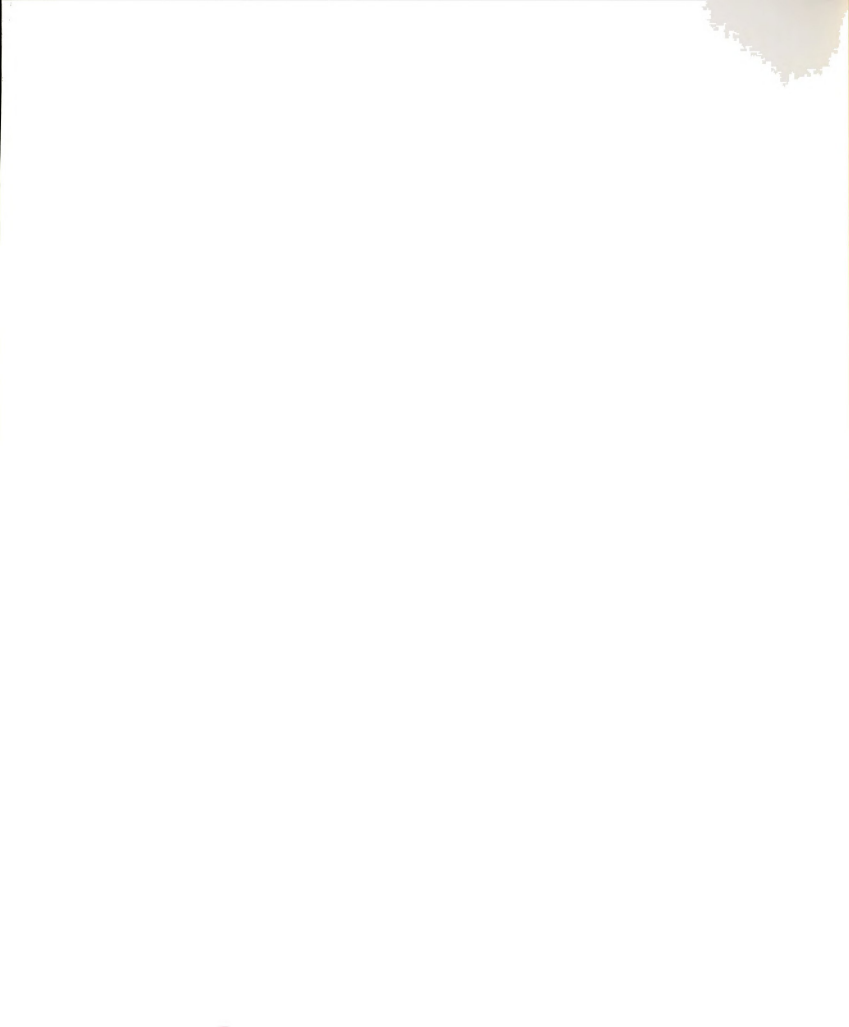
SPEC	DIA mm	CSA mm ²	MAX LD N	DEF mm	k gro N/mm	k phy N/mm	
6L 7R 8R 9L 10L 11L 12R 13L 14L	45.55 55.25 50.45 51.25 53.10 54.68 46.70 49.14 48.05 54.13	1629.5 2397.5 1999.0 2062.9 2214.5 2348.3 1712.9 1896.5 1813.3 2301.3	2634.4 4067.3 1664.3 3026.0 2358.5 2500.9 1468.5 1953.6 1797.8 2225.0	10.67 15.24 13.92 14.11 14.37 15.13 10.72 11.89 11.67 17.97	250.2 177.0 111.3 158.1 148.8 113.4 132.0 129.5 162.7 110.8	328.3 431.9 92.5 869.3 186.5 441.8 163.3 417.1 172.4 241.3	
MAX	55.25	2397.5	4067.3	17.97	250.2	869.3	
MIN	45.55	1629.5	1468.5	10.67	110.8	92.5	
VAR	10.62	67113	523092	4.86	1611	45858	
DEV	3.26	259.1	723.3	2.20	40.1	214.1	
AVG	50.83	2037.6	2369.6	13.57	149.4	334.4	

Table 8. Double Fixation Test Data

SPEC	DIA mm	CSA mm ²	MAX LD N	DEF mm	k gro N/mm	k phy N/mm
6R 7L 8L 9R 10R 11R 12L 13R 14R 15R	46.00 55.85 49.65 50.70 52.58 54.50 46.38 48.65 47.73 53.85	1661.9 2449.8 1936.1 2018.9 2171.4 2332.8 1689.5 1858.9 1789.3 2277.5	3293.0 3884.9 2282.9 2794.6 3115.0 3417.6 3021.6 2652.2 3858.2 2856.7	12.70 15.42 13.72 14.00 14.48 15.02 12.24 13.07 14.94 16.15	253.6 218.0 178.4 162.7 177.4 202.0 212.7 141.0 249.5 139.2	169.7 492.9 243.5 783.4 294.4 338.2 537.3 694.3 258.9 494.3
MAX	55.85	2449.8	3884.9	16.15	253.6	783.4
MIN	45.55	1629.5	2282.9	12.24	139.2	169.7
VAR	10.79	68423	235289	1.42	1494	37296
DEV	3.28	261.6	485.1	1.19	38.7	193.1
AVG	50.71	2028.1	3117.6	14.17	193.5	430.7



APPENDIX B



APPENDIX B

Table 9. Single Screw ANSYS Finite Element Code

```
ANSYS
/INTER, NO
/PREP7
/TITLE, SCFE SINGLE SCREW FIXATION
ET.1.45
EX,1,780
NUXY, 1, 0.14
ET.2.45
EX, 2, 190E3
NUXY, 2, 0, 305
LOCAL, 11, 1
/SHOW, 4105
N. 1
N.2.2.25
N, 3, 9.8
N, 4, 25
NGEN, 8, 3, 2, 4, 1, , 45
NGEN, 4, 25, 1, 25, 1, , , 25
NGEN, 2, 100, 1, 25, 1, , , 76
NGEN, 2, 150, 1, 25, 1, , , 100
TYPE, 2
E, 1, 2, 5, 26, 27, 30
EGEN, 3, 25, 1
E, 1, 5, 8, 26, 30, 33
EGEN, 3, 25, 4
E, 1, 8, 11, 26, 33, 36
EGEN, 3, 25, 7
E, 1, 11, 14, 26, 36, 39
EGEN, 3, 25, 10
E.1,14,17,26,39,42
EGEN, 3.25.13
E,1,17,20,26,42,45
EGEN, 3, 25, 16
E, 1, 20, 23, 26, 45, 48
EGEN, 3, 25, 19
E, 1, 23, 2, 26, 48, 27
EGEN, 3, 25, 22
E, 76, 77, 80, 126, 127, 130
E, 76, 80, 83, 126, 130, 133
E, 76, 83, 86, 126, 133, 136
E, 76, 86, 89, 126, 136, 139
```

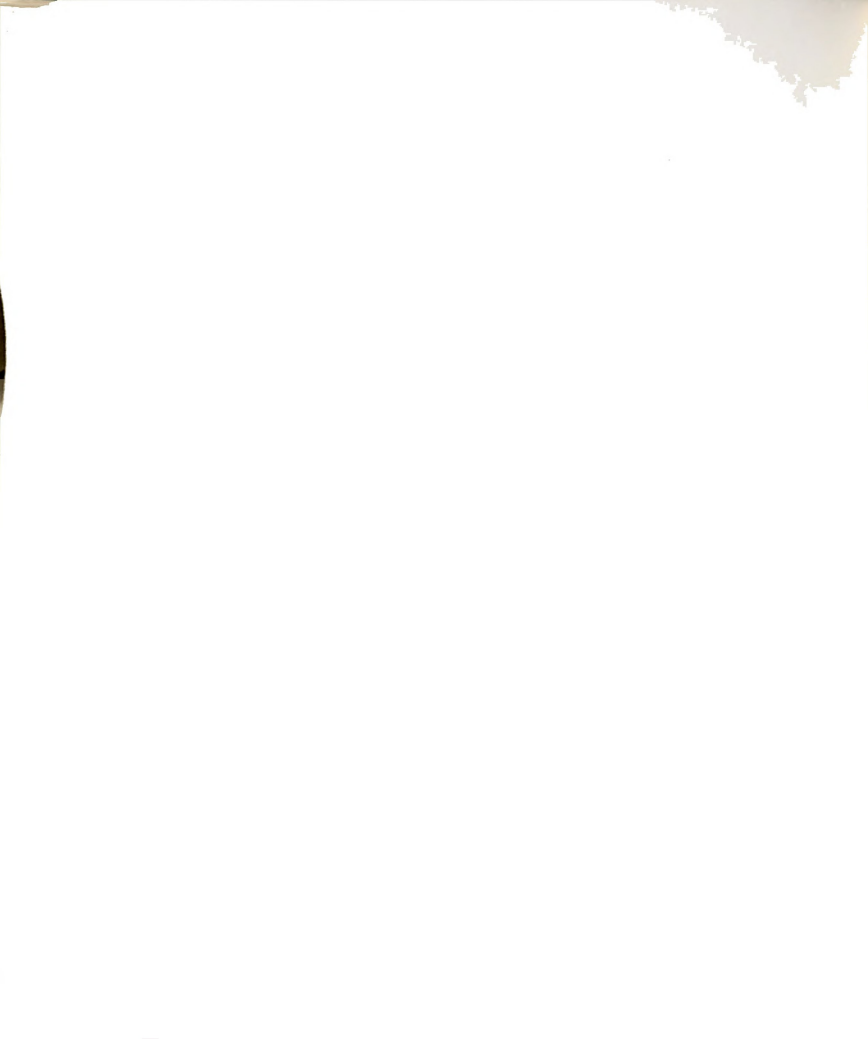


Table 9 (cont'd.)

```
E, 76, 89, 92, 126, 139, 142
E, 76, 92, 95, 126, 142, 145
E, 76, 95, 98, 126, 145, 148
E, 76, 98, 77, 126, 148, 127
TYPE, 1
E, 2, 3, 6, 5, 27, 28, 31, 30
EGEN, 6, 25, 33
E, 3, 4, 7, 6, 28, 29, 32, 31
EGEN, 6, 25, 39
E,5,6,9,8,30,31,34,33
EGEN, 6, 25, 45
E, 6, 7, 10, 9, 31, 32, 35, 34
EGEN, 6, 25, 51
E, 8, 9, 12, 11, 33, 34, 37, 36
EGEN, 6, 25, 57
E, 9, 10, 13, 12, 34, 35, 38, 37
EGEN, 6, 25, 63
E, 11, 12, 15, 14, 36, 37, 40, 39
EGEN, 6, 25, 69
E, 12, 13, 16, 15, 37, 38, 41, 40
EGEN, 6, 25, 75
E, 14, 15, 18, 17, 39, 40, 43, 42
EGEN, 6, 25, 81
E, 15, 16, 19, 18, 40, 41, 44, 43
EGEN, 6, 25, 87
E, 17, 18, 21, 20, 42, 43, 46, 45
EGEN, 6, 25, 93
E, 18, 19, 22, 21, 43, 44, 47, 46
EGEN, 6, 25, 99
E, 20, 21, 24, 23, 45, 46, 49, 48
EGEN, 6, 25, 105
E, 21, 22, 25, 24, 46, 47, 50, 49
EGEN, 6, 25, 111
E, 23, 24, 3, 2, 48, 49, 28, 27
EGEN, 6, 25, 117
E, 24, 25, 4, 3, 49, 50, 29, 28
EGEN, 6, 25, 123
EDEL, 36, 128, 6
ECOMPR
YES
```

E,126,127,130,151,152,155 E,126,130,133,151,155,158 E,126,133,136,151,158,161 E,126,136,139,151,161,164 E,126,139,142,151,164,167 E,126,142,145,151,167,170 E,126,145,148,151,170,173 E,126,144,127,151,173,152



WSTART WAVES

- ITER, 1, 1, 1

D,4,ALL,,,25,3 D,29,ALL,,,50,3 D,54,ALL,,,75,3 D,79,ALL,,,100,3

D,104,UY,-6.0,,116,3 D,129,UY,-6.0,,141,3 D,154,UY,-6.0,,166,3

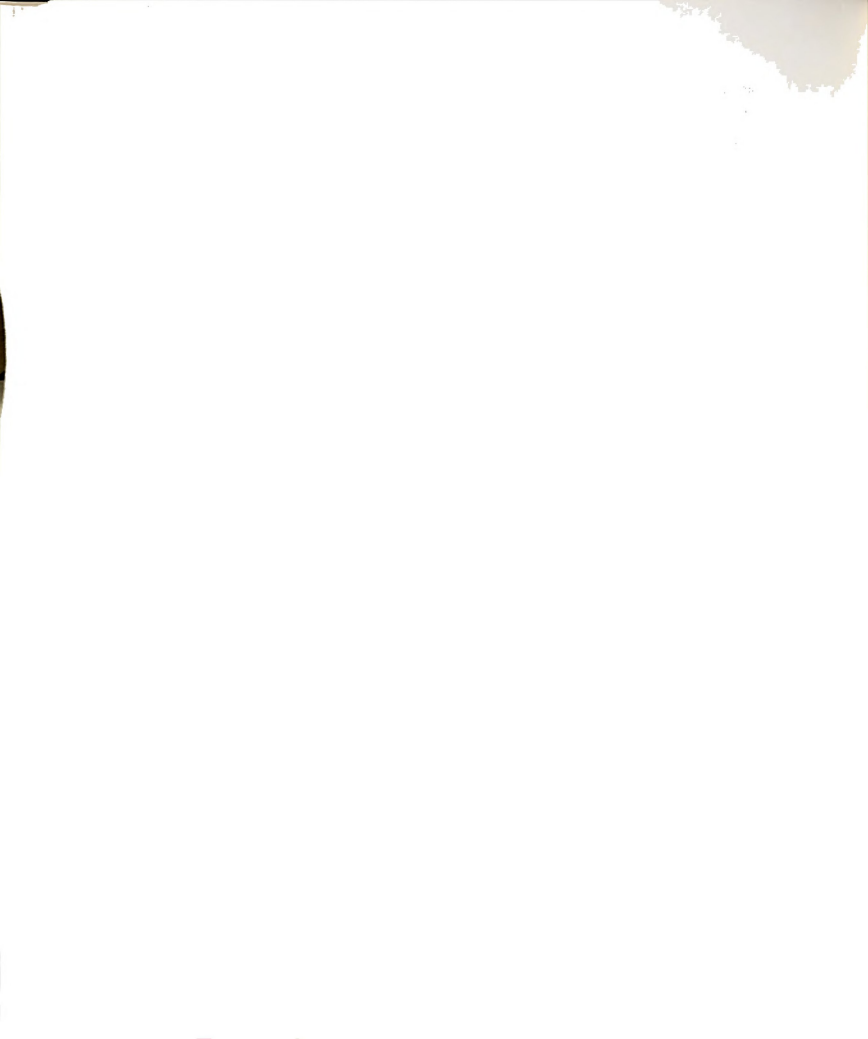


Table 10. Double Screw ANSYS Finite Element Code

```
ANSYS
/INTER, NO
/PREP7
/TITLE, SCFE DOUBLE SCREW FIXATION
ET, 1, 45
EX,1,780
NUXY, 1, 0.14
ET, 2, 45
EX, 2, 190E3
NUXY, 2, 0.305
LOCAL, 11, 1
/SHOW, 4105
N. 1
N, 2, 12.5
N, 3, 25
NGEN, 8, 2, 2, 3, 1, , 45
N, 18, 25, 22.5
N, 19, 25, 157.5
N, 20, 25, 202.5
N, 21, 25, 337.5
LOCAL, 11,0
N, 22, 7.25
N.23,9.5
N, 24, 8.841, 1.591
N, 25, 7, 25, 2, 25
N, 26, 5.659, 1.591
N, 27, 5
N, 28, 5, 659, -1, 591
N, 29, 7.25, -2.25
N,30,8.841,-1.591
N, 31, 10.9622, 3.1723
N, 32, 3.625, 3.625
N, 33, 0, 5.1625
SYMM, 2, 3, 31
SYMM, 2, 3, 32
SYMM, 2, 3, 33
SYMM, 1, 15, 22, 30
SYMM, 1, 15, 31, 36
NDEL, 48
NDEL, 51
SYMM, 2, 2, 46
```



Table 10 (cont'd.)

NDEL, 49 SYMM, 2, 2, 47 NDEL, 50

NGEN,4,49,1,49,1,,,25 NGEN,2,196,1,49,1,,,76 NGEN,2,245,1,49,1,,,90 NGEN,2,294,1,49,1,,,100

TYPE, 2

E.22,23,24,71,72,73 EGEN, 3, 49, 1 E, 22, 24, 25, 71, 73, 74 EGEN, 3, 49, 4 E, 22, 25, 26, 71, 74, 75 EGEN, 3, 49, 7 E, 22, 26, 27, 71, 75, 76 EGEN, 3, 49, 10 E, 22, 27, 28, 71, 76, 77 EGEN, 3, 49, 13 E, 22, 28, 29, 71, 77, 78 EGEN, 3, 49, 16 E, 22, 29, 30, 71, 78, 79 EGEN, 3, 49, 19 E, 22, 30, 23, 71, 79, 72 EGEN, 37, 49, 22

E,169,170,171,267,268,269 E,169,171,172,267,269,270 E,169,172,173,267,270,271 E,169,173,174,267,271,272 E,169,174,175,267,272,273 E,169,176,177,267,273,274 E,169,176,177,267,274,275 E,169,177,170,267,273,274

ESYM, 2, 15, 1, 32

TYPE, 1

E,1,36,35,50,85,84 EGEN,6,49,65 E,36,14,16,35,85,63,65,84

EGEN, 6, 49, 71 E, 14, 15, 17, 16, 63, 64, 66, 65 EGEN, 6, 49, 77 E, 1, 35, 28, 27, 50, 84, 77, 76 EGEN, 6, 49, 83

E, 35, 16, 29, 28, 84, 65, 78, 77



EGEN, 6, 49, 89

E, 29, 16, 34, 30, 78, 65, 83, 79 EGEN, 6, 49, 95 E, 30, 34, 2, 23, 79, 83, 51, 72 EGEN, 6, 49, 101 E, 16, 17, 21, 34, 65, 66, 70, 83 EGEN, 6, 49, 107 E, 34, 21, 3, 2, 83, 70, 52, 51 EGEN, 6, 49, 113 E, 1, 27, 26, 32, 50, 76, 75, 81 EGEN, 6, 49, 119 E, 32, 26, 25, 4, 81, 75, 74, 53 EGEN, 6, 49, 125 E, 4, 25, 24, 31, 53, 74, 73, 80 EGEN, 6, 49, 131 E, 24, 23, 2, 31, 73, 72, 51, 80 EGEN, 6, 49, 137 E, 31, 2, 3, 18, 80, 51, 52, 67 EGEN, 6, 49, 143 E, 4, 31, 18, 5, 53, 80, 67, 54 EGEN, 6, 49, 149 E,1,32,33,50,81,82 EGEN, 6, 49, 155 E, 33, 32, 4, 6, 82, 81, 53, 55 EGEN, 6, 49, 161 E, 6, 4, 5, 7, 55, 53, 54, 56 EGEN, 6, 49, 167 E, 1, 33, 47, 50, 82, 96 EGEN, 6, 49, 173 E, 8, 47, 33, 6, 57, 96, 82, 55 EGEN, 6, 49, 179 E, 9, 8, 6, 7, 58, 57, 55, 56 EGEN, 6, 49, 185 E, 1, 47, 41, 42, 50, 96, 90, 91 EGEN, 6, 49, 191 E, 41, 47, 8, 40, 90, 96, 57, 89 EGEN, 6, 49, 197 E, 40, 8, 46, 39, 89, 57, 95, 88 EGEN, 6, 49, 203 E, 39, 46, 10, 38, 88, 95, 59, 87 EGEN, 6, 49, 209 E, 8, 9, 19, 46, 57, 58, 68, 95 EGEN, 6, 49, 215 E, 46, 19, 11, 10, 95, 68, 60, 59 EGEN, 6, 49, 221 E,1,42,43,49,50,91,92,98

EGEN,6,49,221 E,1,42,43,49,50,91,92,98 EGEN,6,49,227 E,43,44,12,49,92,93,61,98 EGEN,6,49,233 E,44,45,48,12,93,94,97,61

```
EGEN, 6, 49, 239
```

E, 45, 38, 10, 48, 94, 87, 59, 97

EGEN, 6, 49, 245 E, 10, 11, 20, 48, 59, 60, 69, 97 EGEN, 6, 49, 251 E, 48, 20, 13, 12, 97, 69, 62, 61 EGEN, 6, 49, 257 E, 1, 49, 36, 50, 98, 85 EGEN, 6, 49, 263 E, 49, 12, 14, 36, 98, 61, 63, 85 EGEN, 6, 49, 269 E, 12, 13, 15, 14, 61, 62, 64, 63 EGEN, 6, 49, 275

EDEL, 68, 280, 6 ECOM

E,267,268,269,316,317,318 E,267,269,270,316,318,319 E,267,270,271,316,319,320 E,267,271,272,316,320,321 E,267,272,273,316,321,322 E,267,272,273,316,322,323 E,267,274,275,316,322,323 E,267,274,275,316,323,324 E,267,275,268,316,323,324

ESYM, 2, 15, 245, 252

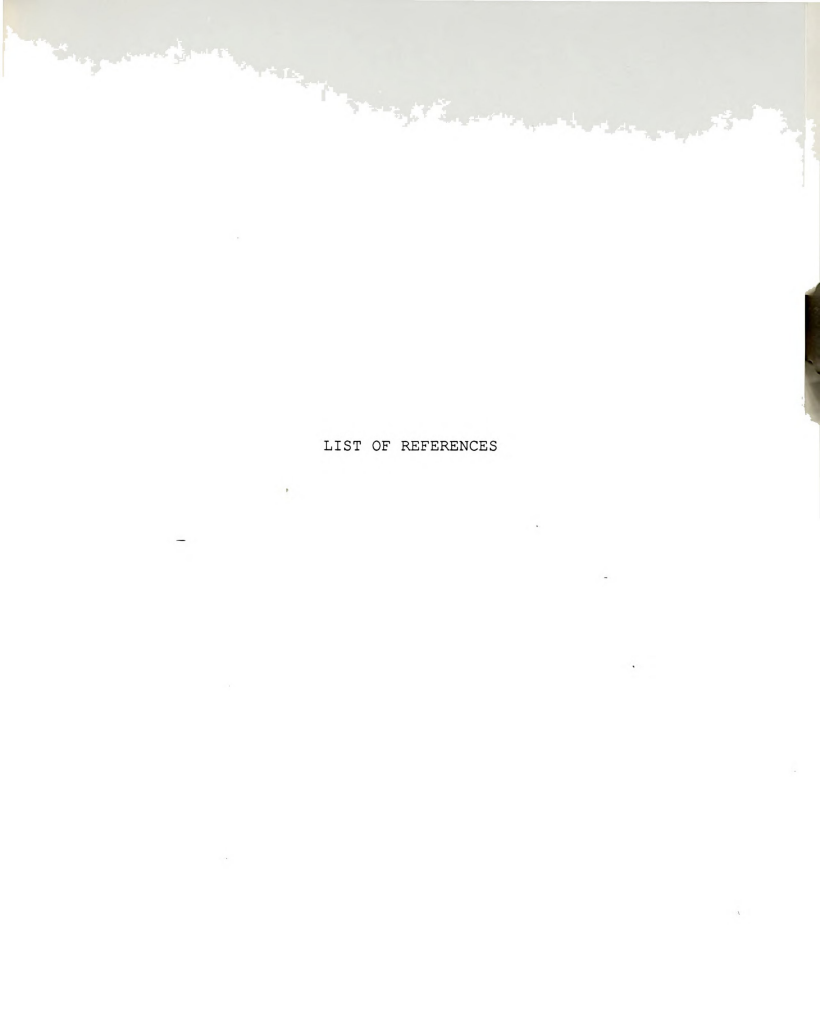
WSTART, 1, 49 WAVES

ITER, 1, 1, 1

D,3,ALL,,,17,2 D,52,ALL,,,66,2 D,101,ALL,,115,2 D,150,ALL,,164,2 D,18,ALL,,,21,0 D,67,ALL,,,70,0 D,116,ALL,,,119,0 D,165,ALL,,,168,0

D,199,UY,-6.0,,207,2 D,248,UY,-6.0,,256,2 D,297,UY,-6.0,,305,2 D,214,UY,-6.0,,217,0 D,263,UY,-6.0,,266,0 D,312,UY,-6.0,,315,0





- Aronson, D.D., Carlson, W. E. "Single Screw Fixation for Slipped Capital Femoral Epiphysis." <u>Orthopedic</u> Transactions, 1985, p. p. 497.
- Asnis, S.E. "The Guided Screw System in Intracapsular Fractures of the Hip." <u>Contemporary Orthopedics</u>, June, 1985, 10(6), pp. 33-42.
- Beaupre, G.S., Carter, D.R., Orr, T.E. and Csongradi, J. "Stresses in Plated Long Bones: The Role of Screw Tightness and Interface Slipping." <u>The Journal of</u> Orthopedic Research, 1988, 6, pp. 39-50.
- Bennett, G.C., Koreska, J., and Rang, M. "Pin Placement in Slipped Capital Femoral Epiphysis." <u>The</u> <u>Journal of Pediatric Orthopedics</u>, 1984, 4, pp. 574-578.
- Brown, T.D., Way, M.E., Fu, F.H., and Ferguson, A.B. Jr. "Some Femoral Head Load Changes Occurring with Infarction and Normal Growth." <u>Finite Elements in</u> <u>Biomechanics</u>, John Wiley & Sons, Ltd., 1982, pp. 269-293.
- Carey, R.P.L., Moran, P.L., and Cole, W.G. "The Place of Threaded Pin Fixation in the Treatment of Slipped Upper Femoral Epiphysis." <u>Clinical Orthopaedics</u>, November, 1987, No. 224, pp. 45-51.
- Chung, S.M.K., Batterman, S.C., and Brighton, C.T.
 "Shear Strength of the Human Capital Epiphyseal
 Plate." The Journal of Bone and Joint Surgery,
 January, 1976, 58A, No. 1, pp. 94-103.
- Chung, S.M.K., Hirata, T.T. "Multiple Pin Repair of the Slipped Capital Femoral Epiphysis." <u>Clinical</u> Biomechanics, 1981, pp. 94-115.
- DeSalvo, G.J., Gorman, R.W. <u>ANSYS Engineering Analysis System</u> Rev. 4.3, Swanson Analysis Systems, Inc. P.O. Box 65, Houston, Pennsylvania 15342.



- 10. Gelberman, R. H. "The association of Femoral Retroversion with Slipped Capital Femoral Epiphysis." <u>The Journal of Bone and Joint Surgery</u>, September, 1986, 68-A(7), pp. 1000-1007.
- 11. Greenough, C. G., Bromage, J.D., and Jackson, A.M. "Pinning of the Slipped Upper Femoral Epiphysis: A Trouble-Free Procedure?" <u>The Journal of Pediatric</u> Orthopedics, 1985, 5, pp. 657-660.
- 12. Gruebel Lee, D.M. <u>Disorders of the Hip</u>, Philadelphia: J. B. Lippincott Company, 1983, pp. 175-192.
- Hägglund, G., Hannson, L.I., Ordeberg, G., and Sandström, S. "Slipped Capital Femoral Epiphysis in Southern Sweden: Long-term Results after Femoral Neck Osteotomy." <u>Clinical Orthopaedics</u>, September, 1986, 210, pp. 152-159.
- 14. Hägglund, G., Hannson, L.I., and Sandström, S. "Slipped Capital Femoral Epiphysis in Southern Sweden: Long-Term Results after Nailing/Pinning." <u>Clinical Orthopaedics</u>, April, 1987, 217, pp. 190-200.
- Hall, J.E. "The Results of Treatment of Slipped Capital Femoral Epiphysis." <u>Journal of Bone and Joint Surgery</u>, 1957, 39B, pg. 659.
- Hamill, P.V.V., Drizd, T.A., Johnson, C.L., Reed, R.B., Roche, A.F. and Moore, W.N. "Physical Growth: National Center for Health Statistics Percentiles." <u>American</u> <u>Journal of Clinical Nutrition</u>, 1979, 32, pp. 607-629.
- Hamilton, G. F., Turner, A.S., Ferguson, J.G. and Pharr, J.W. "Slipped Capital Femoral Epiphysis in Calves." <u>JAVMA</u>, June, 1978, 172, pp. 1318-1322.
- Herndon, C.H., Heyman, C.H. and Bell, D.M. "Treatment of Slipped Capital Femoral Epiphysis by Epiphysiodesis and Osteoplasty of the Femoral Neck." <u>Journal of Bone</u> and <u>Joint Surgery</u>, 1963, 45A, pg. 999.
- Jerre, T. "Early Complications after Osteosynthesis with a Three-Flanged Nail in situ for Slipped Epiphysis." <u>Acta Orthopedica Scandinavia</u>, 1958, 27, pg. 126.
- Jerre, T. "A Study in Slipped Upper Femoral Epiphysis." <u>Acta Orthopedica Scandinavia</u>, Supplement 6, 1960.



- Kruger, D. M., Hak, D.J., Viviano, D.M., Goldstein, S.A., and Herzenberg, J.E. "Biomechanical Comparison of Single and Double Steinmann Pin Fixation for Slipped Capital Femoral Epiphysis." <u>Proceedings of the</u> Orthopedic Research Society, 1988, pp. 485-6.
- Lehman, W.B., Grant, A., Rose, D., Pugh, J., and Norman, A. "A Method of Evaluating Possible Pin Penetration in Slipped Capital Femoral Epiphysis Using a Cannulated Internal Fixation Device." <u>Clinical Orthopaedics</u>, June, 1984, No. 186, pp. 65-70.
- 23. Litchman, H.M. and Duffy, J. "Slipped Capital Femoral Epiphysis: Factors Affecting Shear Forces on the Epiphyseal Plate." The Journal of Pediatric Orthopedics, November, 1984, 4, No. 6, pp. 745-748.
- Lynch, G.J., and Stevens, D.B. "Slipped Capital Femoral Epiphysis - Treatment by Pinning In Situ." Clinical Orthopaedics, August, 1987, No. 221, pp. 260-266.
- 25. Mann, D. and Weddington, J. "Slipped Capital Femoral Epiphysis: Results of Treatment with a Single Cannulated Screw." Orthopedics, February, 1989, 12, pp. 251-255.
- McAfee, P.C., and Cady, R.B. "Endocrinologic and Metabolic Factors in Atypical Presentations of Slipped Capital Femoral Epiphysis." <u>Clinical Orthopaedics</u>, November, 1983, pp. 188-197.
- 27. <u>Metals Handbook</u>. American Society for Metals, Metals Park Ohio, 1978. Vol. 1, 8th Edition, p. 423.
- Meyers, M.H. <u>Fractures of the Hip</u>. Chicago: Year Book Medical Publishers INC., 1985.
- Moreau, M. J. "Remodeling in Slipped Capital Femoral Bpiphysis." <u>The Canadian Journal of Surgery</u>, November, 1987, 30, No. 6, pp. 440-442.
- Moss, J., Zuelzer, W., and Nogi, J. "Slipped Capital Femoral Epiphysis: A Review of Treatment and Complications." Orthopedic Transactions, 1982, 6(3), pq. 380.
- Natural and Living Biomaterials, CRC Press, Inc., 1984, pp. 91-93.
- Nuzzo, R.M. "A Computer Model of Slipped Capital Femoral Epiphysis. Causes of Fixation Error and Chondrolysis." Orthopedics, January, 1986, 9, No. 1, pp. 79-90.



- 33. O'Brien, E. and Fahey, J. "Remodeling of the Femoral Neck after In Situ Pinning for Slipped Capital Femoral Epiphysis." The Journal of Bone and Joint Surgery, 1977, 59A, No. 62.
 - 34. Ordeberg, G., Hannson, L.I., and Sandström, Sand
 - Ordeberg, G. Hannson, L.I., and Sandström, S. "Slipped Capital Femoral Epiphysis in Southern Sweden: Long-term results after Closed Reduction and Hip Spica." Clinical Orthopaedics, July, 1987, 220, pp. 148-154.
 - Paul, J.P. "Force Actions Transmitted by Joints in the Human Body." <u>Proceedings of the Royal Society of London</u>, Series B, 1976, 192, pp. 163-172.
 - Previte, J.J. <u>Human Physiology</u>, New York: McGraw-Hill, 1983, pp. 343-345.
 - Pritchett, J.W., Perdue, K.D. "Mechanical Factors in Slipped Capital Femoral Epiphysis." <u>Journal of</u> <u>Pediatric Orthopedics</u>, 1988, 8(4), pp. 385-388.
 - Rapperport, D.J., Carter, D.R., and Schurman, D.J. "Contact Finite Element Stress Analysis of Pourous Ingrowth Acetabular Cup Implantation, Ingrowth, and Loosening. The Journal of Orthopedic Research, 1987, 5, pp. 548-561.
 - Schwartz, M.H. "A Finite Element Analysis of Plated Long Bones." Master's Thesis, Michigan State University, East Lansing, MI., 1988.
 - 41. Shigley, J.E., Mitchell, L.D. <u>Mechanical Engineering Design</u>. McGraw-Hill, Inc., 1983, p. 808.
 - Stambough, J.L., Davidson, R.S., Ellis, R.D., and Gregg, J.R. "Slipped Capital Femoral Epiphysis: An Analysis of 80 Patients as to Pin Placement and Number." <u>The Journal of Pediatric Orthopedics</u>, May, 1986, 6, No. 3, pp. 265-273.
 - Swiontkowski, M.F. Slipped Capital Femoral Epiphysis: Complications Related to Internal Fixation. Orthopedics, June, 1983, 6, pp. 705-712.
 - Swiontkowski, M.F., and Gill, E.A. "Slipped Capital Femoral Epiphysis." <u>American Family Physician</u>, April 1986, pp. 167-171.

- 45. Tönnis, D. Congenital Dysplasia and Dislocation of the Hip. Berlin: Springer-Verlag, 1987, pp. 1-56.
- Walters, R., Simon, S.R. "Joint Destruction: A Sequel of Unrecognized Pin Penetration in Patients with SCFE." <u>Preceedings of the Eighth Meeting of the Hip Society</u>, 1980, pg. 145.
- Wilson, P.D., Jacobs, B. and Schecter, L. "Slipped Capital Femoral Epiphysis: An End-Result Study." Journal of Bone and Joint Surgery, 1965, 47A, pg. 1128
- 48. Zahrawi, F.B., Stephens, T.L., Spencer, G.E., and Clough, J.M. "Comparative Study of Pinning <u>In situ</u> and Open Epiphysiodesis in 105 Patients with Slipped Capital Femoral Epiphyses." <u>Clinical Orthopaedics</u>, July, 1983, No. 177, pp. 160-168.







